



Published in final edited form as:

*Sens Actuators A Phys.* 2021 August 01; 326: . doi:10.1016/j.sna.2021.112602.

## A review of peristaltic micropumps

Farzad Forouzandeh<sup>\*</sup>, Ahmed Alfadhel, Arpys Arevalo, David A. Borkholder

Microsystems Engineering, Rochester Institute of Technology, Rochester, NY, USA

### Abstract

This report presents a review of progress on peristaltic micropumps since their emergence, which have been widely used in many research fields from biology to aeronautics. This paper summarizes different techniques that have been used to mimic this elegant physiological transport mechanism that is commonly found in nature. The analysis provides definitions of peristaltic micropumps and their different features, distinguishing them from other mechanical micropumps. Important parameters in peristalsis are presented, such as the operating frequency, stroke volume, and various actuation sequences, along with introducing design rules and analysis for optimizing actuation sequences. Actuation methods such as piezoelectric, motor, pneumatic, electrostatic, and thermal are discussed with their advantages and disadvantages for application in peristaltic micropumps. This review evaluates research efforts over the past 30 years with comparison of key features and outputs, and suggestions for future development. The analysis provides a starting point for researchers designing peristaltic micropumps for a broad range of applications.

### Keywords

Peristaltic; Micropump; Microfluidics; MEMS; Drug delivery; Lab-on-a-chip

## 1 Introduction

In recent decades, microsystem technologies have made significant progress, and impacted various fields such as biology, biomedical engineering, biochemistry research, among other research areas. Micropumps are the heart of microfluidics systems since they provide the necessary power for moving the working fluid. In this work, we use the definition of micropump according to [1], where the prefix ‘micro’ is considered to be appropriate for devices with prominent features having space dimension scale in the order of hundreds of microns or smaller. Most micropumps can be categorized into two groups: mechanical micropumps (with moving parts) and non-mechanical micropumps (with no moving parts) [1–3]. Mechanical micropumps employ reciprocating pistons or oscillating diaphragms to do pressure work on the working fluid through a deformable and moving boundary in the pumping chamber, while rectification components such as active or passive valves at the inlet and outlet control the flow direction.

---

<sup>\*</sup>Corresponding author at: Microsystem Engineering, Kate Gleason College of Engineering, Rochester Institute of Technology, 168 Lomb Memorial Drive, Rochester, NY 14623, USA. ff7667@rit.edu.

Peristalsis is one of the essential physiological transport mechanisms in living organs and organisms, enabling functions such as digestive tract, urethral transport, blood flow in the circulatory system, etc. This elegant transport mechanism has inspired researchers to investigate the applicability of peristaltic pumping in the realm of microfluidic devices. In the literature, peristaltic micropumps (PMPs) are often listed as a subcategory of mechanical micropumps, typically with three or more pumping chambers that operate in a particular sequence to push a working fluid in a desired direction within a microfluidic path [1,3–6]. The first PMP was introduced by Smits in 1990, using microelectromechanical systems (MEMS) fabrication techniques. The device had a set of three piezoelectric actuators, which used a six-step sequence to create a peristalsis transport mechanism [7]. This micropump had a maximum flow rate ( $Q_{max}$ ) of 3  $\mu\text{L}/\text{min}$  and a maximum differential pressure ( $P_{max}$ ) of 5.9 kPa.

Since the introduction of PMPs, they have been widely used in various microfluidic applications such as cell sorting/counting and cytometry [8], DNA hybridization [9], gas chromatography [10], droplet microfluidics [11], particle and cell separation [12–14], cell culture and multi-organ-chip [9,15–17], blood transportation [18], on-chip rapid mixing [19], morphine detection [20], aeronautics [21], biosampling for disease detection [22], implanted artificial sphincter system [23], detection of *Salmonella* spp. in food samples [24], parallel processing of cell cultures and DNA microarrays [25], and plug-and-play microfluidic chips [26]. Further, PMPs have been designed and used for drug delivery, such as implantable drug delivery systems [27–29], inner ear drug delivery [30–34] (reviewed recently in [35]), high-resolution volumetric dosing [36], and insulin delivery [37]. Key features that make PMPs attractive for drug delivery applications are resistance to high backpressure, bubble tolerance, endurance, and self-priming and bi-directional flow capabilities.

This review introduces the peristalsis transport mechanism concept and defines the different configurations that exist in the literature. This is followed by a discussion on the effect of most critical parameters for the functionality of PMPs along with rules of thumb for operation optimization. The different actuation methods that have been used to achieve such devices are presented with selected examples addressing challenges for their application in PMPs. Finally, the review closes with a discussion, comparison, and evaluation of the developed PMPs over the past 30 years along with suggestions for future directions to improve PMPs for broader applications.

## 2 Peristaltic micropump definition and classifications

PMPs are mechanical micropumps that drive the working fluid from the inlet to outlet with a traveling wave without using rectification components (e.g., valves). However, in the literature, PMPs are frequently categorized either as a subcategory of mechanical micropumps listed as an actuation method or vaguely explained among other micropumps [1,2,5,38,39]. Since in PMPs the actuator(s) are the only components to rectify the flow, this review considers peristalsis as a rectification method for mechanical micropumps [3]. Table 1 shows a categorized summary of typical rectification methods for mechanical micropumps. In this review, PMPs with side chambers overlapping inlet and outlet ports

(See Table 2A, bottom) are considered PMPs if the side chambers are substantially similar (in stroke volume, actuation method, etc.) to the middle chamber(s); a categorization that has been used in the literature [3,7,40–43]. In this review actuators and actuation sites (chambers) are distinguished since in some PMPs they are not at the same location and a transmission mechanism connects them for different purposes.

PMPs can be categorized by the fluidic channel configuration either as a continuous-channel or discrete-channel PMP. A continuous-channel PMP design has its actuators fabricated around or along a single-compartment continuous microfluidic channel, such as a microtubing, while a discrete-channel PMP is composed of two or more layers to create a microfluidic channel. Typically, discrete-channel PMPs are designed with ports to connect to other elements in relatively larger systems. The multi-layer design approach used for the discrete-channel PMPs usually increases the complexity of the fabrication. This introduces challenges that need to be addressed for a successful device fabrication such as having a strong bond between layers to seal the microchannels and to avoid leakage within the device, layers alignment, channel clogging and addition of port interconnections. The latter is especially challenging for size-constrained applications, necessitating complex fabrication approaches to realize robust microfluidic interconnections to the discrete channel PMPs (e.g., [44]).

Actuation direction of the PMPs can also be classified into two general schemes regarding the transportation of the fluid: continuous and discrete. In the continuous-scheme PMPs the fluid is actuated along the flow direction (e.g., PMPs with rollers or cams [19,37] while in the discrete-scheme the fluid is actuated perpendicular to flow direction (e.g., [45–50]. In other words, in continuous and discrete -scheme PMPs the traveling wave is generated by actuation of infinite and finite sites of the fluidic channel, respectively (see Table 2). The operational concept of continuous-scheme PMPs is usually based on the miniaturization of peristaltic pumps. Although the continuous-scheme concept of PMPs has been improved in the past two decades, most of the PMPs in the literature are discrete-scheme, which fits well with the microscale fabrication processes (e.g., MEMS) and actuation methods.

Discrete-scheme PMPs are usually defined as micropumps with three or more pumping chambers, with one actuator for each [1,5] (Table 2A). These are the most common type of discrete-scheme PMPs. However, to reduce the device footprint, failure potentials, and complications of multiphase excitation controllers for multiple actuators [5,51,52], researchers have investigated PMPs with fewer actuators. One of the first two-actuator PMPs was introduced by Berg et al. in 2003 [51], with a structure similar to Table 2B. In this study, two pneumatic-driven PMPs were developed using two and three actuators, while other parameters remain identical. The results show that a two-chamber PMP can provide up to 94% of the flow rate and 73% of the  $P_{max}$  of the counterpart three-chamber PMP. The results suggest that two-stage PMPs may be a more viable choice in limited chip area conditions, or where the backpressure is low. Another study reported a backpressure-independent piezoelectric PMP designed for a low flow rate range of 0.1–50  $\mu\text{L}/\text{min}$  using two chambers [53]. Single-actuator PMPs (SAPMPs) are discrete-scheme PMPs that employ one actuator to sequentially actuate multiple chambers with an engineered delaying transmission mechanism [54,55] (Table 2C). These SAPMPs are typically pneumatic-driven

[54–58]. Peristalsis is created by a delaying transmission mechanism for sequentially closing and opening the chambers, due to different fluidic resistances between the actuator and chambers or different volumes of driving chambers.

In Continuous-scheme PMPs the pumping chamber actuates the working fluid in two configurations: (i) The actuator and the transmission mechanism move along the flow direction. Most of these PMPs are motor-driven, typically with roller-based, cam-follower, or magnetic transmission mechanism. (ii) The actuator moves perpendicular to the flow direction, while a transmission mechanism converts the actuation to a travelling wave along the flow direction. DC-motors [59] and piezoelectric [52,60,61] actuation methods have been used for driving these PMPs. A perpendicular-to-parallel (*PtP*) conversion has been realized by engineering geometrical or mechanical properties of the diaphragm [60], loosely attached actuator with asymmetric location of inlet and outlet ports [52], or a mechanical mechanism [59].

### 3 Significant parameters in peristalsis

Many researchers explored the effect of different parameters on the operation of the PMPs, including the operating frequency, the number of chambers, operating sequence, phase difference, and the working fluid [42,62–66]. Flow rate of a PMP can be formulated by Equation (1):

$$Q = V_{cycle} \times f \quad (1)$$

Where  $Q$ ,  $V_{cycle}$  and  $f$  stand for flow rate, net pumped volume in a single cycle, and the number of cycles in each unit of time (operating frequency,  $f$ ), respectively. This section explores significant parameters that define the flow rate by impacting  $V_{cycle}$  and  $f$ , which in some cases can be interrelated.

#### 3.1 Operating frequency

One of the best post-fabrication tools to control a PMP is the tuning of the operating frequency. A noticeable characteristic behavior can be observed among several variations of PMPs investigated in this study: the flow rate increases almost linearly with the increase of the operating frequency in the relatively low-frequency range, followed by a maximum flow rate (at  $f_{Qmax}$ ), and then the flow rate decreases with a further increase of the operating frequency. Figure 1 shows this trend among nine different PMPs with various actuation methods. The average line clearly shows this behavior, which is consistent with the graphs reported elsewhere [38], suggesting that this is expected from all micropumps and not just PMPs.

This relation enables an effective and reliable way of controlling the flow rate at frequencies smaller than  $f_{Qmax}$ . In this range the duration of each cycle is long enough to let the chambers fully close/open, delivering full stroke volume ( $V_{st}$ ). It is worth noting that depending on the micropump characteristic, even if the full stroke volume is not pumped, the faster actuation can compensate and result in increased flow rate. At frequencies higher than

$f_{Q_{max}}$  flow saturation takes place due to reasons including working fluid viscosity [7] and chambers opening and closing time [67,68]. We recommend operating PMPs in actuation frequencies in which the full  $V_{st}$  is pumped to make  $V_{cycle}$  independent of  $f$  to minimize variables, resulting in a better control over the flow rate. For PMPs that operate with compressible working fluids (e.g., air) further considerations should be taken into account which are discussed elsewhere [69].

### 3.2 Stroke volume

Stroke volume ( $V_{st}$ ) is defined as the volume of the working fluid being swept by each chamber in one actuation. In other words, stroke volume is the difference between the maximum and minimum chamber volume ( $V_{max} - V_{min}$ ) as the membrane actuates once.  $V_{st}$  is often impacted by pump geometry, the interaction of solid and fluid mechanics of the pump, and operating frequency (see section 3.1). As a rule of thumb, the parameters in the equation for membrane deflection (Young's modulus, Poisson ratio, membrane thickness and diameter, and net pressure applied which includes actuation pressure and backpressure) and Poiseuille equation (fluid viscosity, net pressure, microchannel dimensions) should be considered. Further,  $V_{min}$  is also impacted by the dead volume which is defined as the volume in a chamber that is not swept by the membrane. Although insightful generic models for micropumps and PMPs are presented in [1,42], subjective modeling for pump design using low-order lumped models and computational modeling are recommended.

Several of these parameters have been considered by researchers in analytical and experimental approaches. Wang and Lee reported the effects of actuation pressure in a pneumatic-driven S-shaped SAPMP [55]. They demonstrated that an increase in the driving pressure by 1.5 times raised the  $Q_{max}$  by 42%, due to increased deflection of the membrane, and therefore,  $V_{st}$  which results in increased  $Q_{max}$ . However, by further increase in the driving pressure,  $Q_{max}$  does not change significantly, since the membrane is already fully deflected. Similarly, Lee et al. reported that in their piezoelectric PMP a 50% increase in the driving voltage causes 117% increase in the  $Q_{max}$  due to elevated  $V_{st}$  [70]. They also simulated the effect of membrane thickness on its deflection which directly affects  $V_{st}$ . The results demonstrate up to 4 times reduction in membrane deflection due to 6 times increase in the thickness.

In modular designs where changing the stroke volume could be as simple as changing one or two elements, tuning stroke volume by changing chamber size can be useful. This idea has been used specifically for continuous PMPs with rollers or ball bearings, where changing the stroke volume by modifying roller or tubing sizes can create a large operating range of flow rate. For example, Koch et al. made a modular design consisting of a PDMS-based or a tubing-based PMP driven by a DC-motor and rollers [71]. They explored different microchannel/microtubing and roller dimensions to demonstrate modularity of the design for covering different flow ranges from 0.5 to 41  $\mu\text{L}/\text{min}$ . Yobas et al. reported a PDMS-based PMP actuated by stainless steel ball bearings that follow the circular shape of a microchannel driven by a permanent magnet mounted on a DC-motor-driven disc [72]. They found that by increasing the roller size by a factor of 2, the flow rate increases by  $\sim 3.5$  times at the same actuation frequencies, enabling a large range of flow rate ( $\sim 10 - 350 \mu\text{L}/\text{min}$ ).

In an effort to minimize the dead volume, Lee et al. created a silicon-polyimide (substrate and diaphragm) electrostatic-driven PMP with sloped-wall chambers using detachment lithography technique, instead of vertical walls which is common in the field [73]. They minimized the dead volume by up to 10 times and increased  $V_{st}$  by 2.2 times at the same operating voltage, resulting in a reduction in the minimum operating voltage and power consumption per flow rate of the PMP by ~30% and 10%, respectively.

The effect of working fluid on  $Q_{max}$  was explored in a study by Jeong and Konishi, by testing deionized (DI) water, a mix of DI water and glycerin (glycerin mix), and diffusion pump oil (oil) with viscosities of 1, 5, and 21.7 cP and relative densities (normalized by water density) of 1, 1.04, and 0.94 [74]. The results show relative flow rates (normalized by water) of 1, 0.79, and 0.12 for DI water, glycerin mix, and oil, respectively. This study, among other studies (e.g., [37,59,70,75]) demonstrates that viscosity is the dominant factor for potential impact of the working fluid on  $Q_{max}$ . However, the impact of working fluid viscosity on the pump performance has been eliminated in a continuous-scheme motor-driven PMP with eight rollers [25]. Results demonstrate insignificant change in the flow rate using DI water and a glycerin mix with viscosities of 1 and 23 cP.

### 3.3 Operating sequence and number of chambers

The operating sequence is composed of multiple steps with a specific order in a single actuation cycle to enable peristalsis in a PMP. Each chamber has an ON or OFF state in each step, represented as 1 and 0 in this section. The operating sequence of a PMP directly affects the PMP performance characteristics ( $Q$ ,  $P_{max}$ , power consumption(PW)), as it determines the number of pumped boluses, overall time of a cycle, and number of chambers at ON state. Actuation schemes can be presented in convertible formats of either duty ratio and phase-lag (e.g. [4]) or step and state of chambers. We show our analysis in the latter format. As an example of conversion between these formats, consider a 4-Chamber PMP with duty ratio of 50% and phase-lag of  $\pi/2$ . Chambers 1, 2, 3, and 4 are ON at  $0-\pi$ ,  $\pi/2-3\pi/2$ ,  $\pi-2\pi$ , and  $3\pi/2-2\pi$  and  $0-\pi/2$ . Each  $\pi/2$  represents a step, therefore the sequence can be written in terms of steps and chamber states as: 1001-1100-0110-0011. Although in the literature the subsections of each sequence are sometimes referred to as phase, we use the term step, to avoid confusion with phase-lag. In all sequences mentioned in this section the flow is from left to right. Steps are written with a series of chamber states (1 or 0) with dashes in between to separate them from other steps. In this section we define  $Q_0 = V_{st} / T_0$  for comparing different sequences, where  $T_0$  is the step time.

Researchers have investigated the impact of operating sequence and number of chambers with numerical, computational, and experimental methods [4,10,68,76–79]. Berg et al. introduced a 2-chamber PMP and compared two sequences: (i) 10-01-00 (ii) 01-11-01-00 [51]. Their simple model predicted  $Q_{ii} = 1.5 Q_i$ , closely matching the experimental value  $Q_{ii} = 1.16 Q_i$ . A study by Graf and Bowser compared different actuation sequences for a 3-chamber piezoelectric-driven PMP [80] including these: (i) 010-011-001-101-100-110 (ii) 011-001-100-110, theoretically resulting in  $Q_{ii} = 3 Q_i$ . However, experiments showed the contradictory results of  $Q_{ii} = 0.8 Q_i$  and  $P_{ii} = 0.8 P_i$ . This is due to having at least one chamber closed at all time for (i) while in (ii) between steps 2 (001) and 3 (100) there is

a short transition time where no chamber is closed leaving the entire channel open, which we define as an open channel state. During the open channel state, backflow occurs due to backpressure, which lowers both  $Q$  and  $P$ , a phenomenon that was reported in a similar circumstance in [68].

In an effort to find the impact of the number of chambers ( $n$ ) and actuation sequence on performance of PMPs, Leu et al. developed a numerical model verified by an experimental setup of a PMP with a motor and magnetic transmission to actuate membranes made of PDMS and iron particles [4]. In this study, the number of chambers ranged from 3 to 8 operating at  $f = 1 \text{ Hz}$ . Sequences with 50% duty ratio and phase-lags between  $10^\circ$  to  $120^\circ$  with  $10^\circ$ -steps were applied. The results showed a relatively linear increase in  $Q_{max}$  by increasing  $n$  at different phase-lags (i.e., sequences), suggesting the importance of operating sequence when increasing  $n$ . Another group investigated the effect of  $n$  on  $Q_{max}$ , with a pneumatically-driven SAPMP with an S-shaped compressed air fluid path on top of the working fluid channel [55]. The structure enables peristalsis based on the phase-lag in closing the chambers due to the time it takes for the compressed air to travel through the S-shaped fluidic path, creating a zipping sequence. In a zipping sequence the chambers are closed from left to right (inlet to outlet), all chambers closed, then open from left to right to load the chambers for the next cycle. The results showed increasing  $n$  from 3 to 5 and from 3 to 7 increases  $Q_{max}$  almost linearly ( $R^2 = 0.96$ ) by 10% and 15% relative to 3-chamber pump.

We present a simple analysis of the impact of  $n$  ( $n > 2$ ) and sequence on the performance of discrete-scheme PMPs in terms of three major parameters of  $Q$ ,  $P$ , and  $PW$ . Among numerous possible actuation sequences that a PMP can operate with, a few of them are presented here: high flow rate sequence (*HQS*), high differential pressure sequence (*HDPS*), and ultra-high flow rate sequence (*UHQS*).

In this analysis it is assumed that in a single cycle of each chamber the full  $V_{st}$  is driven, which does not necessarily mean that chamber is fully closed.  $V_{st}$  is considered equal for all chambers, an assumption that can be adjusted if required (e.g., in PMPs with side chambers at the inlet/outlet ports). To reach the best performance (highest  $Q$  and  $P$  at minimum  $PW$ ) a PMP should work with step time ( $T_\theta$ ) that is just large enough to ensure the chambers fully close and open, a system characteristic that is empirically found for each chamber. The operating frequency can be found as  $f = 1/(mT_\theta)$ , where  $m$  is the number of steps in each sequence. Here we predict  $Q_{max}$  for each sequence, however, the operating flow rate of a PMP can be controlled by tuning  $f$ , which was shown to have a relatively linear correlation to  $Q$  (see Figure 1).

$PW$  and the fluidic resistance ( $R$ ) are found based on averaging the number of actuated chambers in a sequence, stated in terms of power consumption and fluidic resistance of each chamber ( $PW_\theta$ ,  $R_\theta$ ).  $R_\theta$  is considered a fixed value for each chamber at the ON state where the entire  $V_{st}$  is delivered. Also,  $PW_\theta$  and  $R_\theta$  for each chamber are considered equal. These assumptions can be adjusted for specific PMPs. To evaluate efficiency of a PMP in terms of power consumed to deliver a unit of flow rate, power flow rate efficiency is defined as  $\zeta =$

$Q/PW$ . This term assists in understanding efficiency of different sequences for pumping the working fluid.

**3.3.1 High flow rate sequence (HQS)**—In this sequence for all numbers of chambers and at all steps, two chambers are closed and the rest are open, making a pattern of ‘10...01’ with the ON chambers sequentially moving from left to right in  $n$  steps ( $m = n$ ) as shown in Figure 2A. This sequence pumps  $n-2$  boluses of fluid during  $t = nT_0$ , resulting in  $Q = (n-2/n)Q_0$ . Since two chambers are ON in this sequence independent of  $n$ ,  $PW = 2PW_0$  and  $R = 2R_0$ . Note that increasing the number of chambers significantly improves  $Q$ , while  $PW$  and  $R$  are constant, resulting in a larger  $\zeta$ . This sequence has been used commonly in the literature (e.g., [33,81]).

**3.3.2 High differential pressure sequence (HDPS)**—To increase  $P$  a sequence with high fluidic resistance is presented at which for each three chambers two of them are ON, creating patterns of series of ‘110’, while the number of steps is fixed at 3 ( $m = 3$ ), resulting in overall time  $= 3T_0$ . This sequence delivers one bolus during each cycle resulting in  $Q = Q_0/3$ , independent of  $n$  (see Figure 2B). However, by increasing the number of chambers,  $R$  and  $PW$  linearly increase ( $R = (2n/3)R_0$  and  $PW = (2n/3)PW_0$ ). With this sequence, increasing the number of chambers results in larger  $P$  and lower  $\zeta$ , making it suitable for high backpressure environments. This sequence has been used rarely in the literature [68].

A comparison of  $Q$  versus  $n$  for the theoretical values of the *HQS* and *HDPS* models and the literature using the same sequences shows a close match (See Figure S1).  $V_{st}$  is either mentioned in the reference or estimated based on chamber dimensions and membrane deflection.  $T_0$  is found at  $f_{Qmax}$  using  $T_0 = 1/m f_{Qmax}$ , which is the closest match to our assumption in the models for  $T_0$  to be large enough for full chamber actuation. Since  $T_0$  is not reported in the references, the calculated  $T_0$  may not be the smallest possible step time, which may explain the discrepancy between theoretical and experimental values. For designing the actuation sequence a trade-off between  $P$ ,  $Q$ , and  $PW$  should be considered. One of the key parameters significantly affecting these factors is open channel state, which was mentioned earlier in this section. In *HQS* and *HDPS* sequences, the open channel state is avoided during transition time between steps.

**3.3.3 Ultra-high flow rate sequence (UHQS)**—In an attempt to increase the flow rate of PMPs, we introduce a new ultra-high flow rate sequence (*UHQS*) based on the zipping sequence with some modifications. In a typical zipping sequence the chambers serially close from inlet to outlet, all closed, and open from inlet to outlet, generating a nominal performance characteristic of  $Q = (n-1/2n)Q_0$  and  $R = (n^2/2n)R_0$ . In this *UHQS* sequence for an  $n$ -chamber PMP, in the first step chamber 1 and  $n$  are closed, and in a second step which is divided into  $n-2$  mini-steps, chambers are sequentially closed from left to right with a minimal delay ( $T_0/n-2$ ) to ensure that chamber  $i$  is closed before chamber  $i+1$ . In step 3 all chambers except 1 and  $n$  are closed, and in step 4 chamber  $n$  is closed, while other chambers open sequentially from inlet to outlet (Figure 2C). This sequence delivers  $n-2$  boluses of the working fluid in  $t = 4T_0$ , resulting in  $Q = (n-2/4)Q_0$  with power consumption of  $PW = n/2 PW_0$  and fluidic resistance of  $R = n/2 R_0$ . This sequence generates an ultra-high



flow rate compared to the two other sequences for  $n > 4$ . In steps 2 and 4 the middle chambers close/open with a minimal delay, rather than at the same time, to avoid potential structural damage or backflow. These steps require precision control over the chamber deformation and timing. These factors suggest that this sequence is preferable for creating PMPs with more than 4 chambers with a precise actuation control. This sequence also can be used for continuous-scheme PMPs with a custom-designed cam-follower transmission mechanism. Although this sequence is inspired by the zipping sequence it does not suffer from the open channel state, which is a major drawback for zipping sequences.

**3.3.4 Summary of sequences**—We suggested three different sequences in this section for different applications of PMPs. Here we compare these sequences in terms of performance characteristics of  $Q$ ,  $P$  (represented as fluidic resistance,  $R$ ), and power flow rate efficiency ( $\zeta$ ) versus number of chambers ( $n$ ). Comparing  $Q$  of these sequences demonstrates that at all numbers of chambers  $Q_{HQS} > Q_{HDPS}$ , as expected (Figure 2D). However, for  $n \leq 4$   $Q_{UHQS}$  is smaller than  $Q_{HQS}$ , and for  $n > 5$   $Q_{UHQS}$  is significantly larger than  $Q_{HQS}$ . Figure 2E shows that at all numbers of chambers  $HDPS$  creates larger fluidic resistance than the other two sequences, resulting in a larger  $P$ . Furthermore, for 5 or more chambers  $R_{UHQS} > R_{HQS}$ . Figure 2F compares flow rate generated per power consumed ( $\zeta$ ) for different sequences, suggesting equal  $\zeta$  for  $HQS$  and  $UHQS$  at all  $n$ , while significantly decreasing for  $HDPS$  for PMPs with more chambers.

## 4 Actuation methods

The actuation method defines the energy source and the mechanism to convert this energy into a displacement of the working fluid. In this section, different actuation methods that have been used in PMPs are described, with a brief definition of the actuation method, transmission mechanisms to transfer the actuation to the working fluid, and major developments in their applications for PMPs. Further details of each actuation method are reviewed elsewhere [1,5,6].

### 4.1 Motors

DC motors are one of the most popular actuation methods due to their simplicity, low operating voltage, and rotational motion enabling peristalsis with reasonably straightforward configurations. This actuation method has been used in peristaltic pumps, and researchers have miniaturized it for realization of PMPs. To transfer the momentum from the motor to the working fluid, various transmission mechanisms have been implemented including roller, cam-follower and magnets. This actuation method allows fabricating PMPs to pump multiple fluids with a single motor, with applications in high-throughput and highly-integrated microfluidics (e.g., [9,25]). Motor-driven PMPs also enable disposable devices where the fluidic channel (e.g., tubing) can be replaced in a cartridge adjacent to the motor and transmission mechanism [82]. This feature enables using a motor-driven PMP for a broad range of flow rates by simply using different channel sizes (e.g., [71]). However, motor-driven PMPs are among larger PMPs typically with a non-planar structure, and usually require complex external mechanisms for proper handling of the rotary motion.

The roller transmission mechanism was used for PMPs to provide continuous-scheme peristalsis [71,83]. In this transmission mechanism the rotary motion of the motor is transferred to the working fluid (usually in a circular channel) with rollers rolling on the fluidic channel, minimizing the mechanical wear. Cam-follower transmission mechanism translates the rotational motion of the motor to the working fluid in a peristaltic way by sequentially pushing the fluid in different locations, providing discrete-scheme peristalsis [37,84,85]. Shkolnikov et al. reported a novel motor-cam mechanism in which a cam drives a plunger arm that provides peristalsis by closing the inlet of a silicone tubing first, pumping the working fluid out, and opening the tubing from the inlet while the outlet is kept closed to enable loading for next cycle [59]. iPRECIO SMP-310R® infusion pumps [86] are miniature PMPs for implantable drug delivery applications [34,87,88], where peristalsis is created by a micromotor driving a cam with seven followers. The micropump is integrated with a microreservoir and is packaged with a battery for power. The micropump is programmable and implantable with 1.7 nL/min resolution with  $Q_{max} = 167$  nL/min with an accuracy of  $\pm 5\%$  under up to 7.8 kPa backpressure.

Magnetic force has been used to transmit the rotational motion of the motor to the working fluid in both discrete and continuous -schemes. For discrete-scheme PMPs magnets are usually mounted on a motor shaft close to the micropump, while pairing magnetic parts are on the membrane which actuate sequentially when the motor rotates [4,72,89–92]. For continuous-scheme PMPs, a permanent magnet mounted on a motor moves along the fluidic channel that attracts plugs of magnetic fluid or solid pairs to propel the working fluid [93–96].

## 4.2 Piezoelectric

Piezoelectric actuation method works based on an internal mechanical stress induced by an applied electric potential. This actuation method usually does not have a transmission mechanism between the actuators and chambers. The piezoelectric actuators are usually bonded to the actuation membranes in formats of discs [36,43,53,70,76,97–100], cantilevers [26,80,101,102], and bulk and stacks [27,103]. Typically, piezo-driven PMPs are discrete-scheme with multiple actuators on membranes that sequentially actuate and enable peristalsis (e.g., [23,104]). This actuation method is fast and exerts large forces with a planar and relatively simple structure, however, requires high voltage and complicated driving circuit and has a small membrane deflection relative to the footprint (stroke). The displacement of the membrane in piezo-driven PMPs is a function of different parameters including operating frequency and voltage [18], which should be considered by the designers.

Nakahara et al. reported the first piezo-driven SAPMP using a traveling wave concept [60]. In this design, a single cantilever-type piezoelectric stimulates an encapsulated incompressible fluid perpendicular to the flow. The perpendicular actuation generates a traveling wave parallel to the flow which enables peristalsis. A hydraulic displacement amplification mechanism is used to amplify the amplitude of the displacement waves, enabling 1500  $\mu\text{L}/\text{min}$  maximum flow rate. Pe ar et al. reported a single-actuator single-chamber piezoelectric PMP with a PDMS structure [52]. In this design, the inlet port is

placed in one end of the chamber, slightly toward the center, while the outlet port is placed at the other end of the chamber. During the excitation, the loosely attached glass membrane and PDMS deform in a controlled manner, creating a traveling wave from inlet to outlet to enable peristalsis. The micropump provided  $Q_{max} = 240 \mu\text{L}/\text{min}$  and  $P_{max} = 36 \text{ kPa}$ . Cazorla et al. employed  $1.5 \mu\text{m}$  thick Sol-gel PZT thin films for piezoelectric actuation, which reduces the driving voltage down to 24 V, optimized for implantable drug delivery applications [28].

### 4.3 Pneumatic

Pneumatic-driven PMPs use fluctuations in the supply gas (typically air or N<sub>2</sub>) pressure to actuate the membrane exposed to it. This actuation method has been used in PMPs typically with compressed air or vacuum actuators and microfluidic channels/tubings to transmit the actuation to driver chambers adjacent to the working chambers, with solenoid valves to switch and cycle the actuation [40,51,74,105–110]. This actuation method generates large stroke with an easily controllable actuation force with a soft-lithography-friendly fabrication process and small footprint. However, the membrane response is slow, and it typically requires external compressed air sources and control valves that increases the overall size and causes challenges for portability of the device.

To minimize the device volume and facilitate control, pneumatic-driven SAPMPs were developed where peristalsis occurs due to a delaying transmission mechanism creating phase-lag between the chambers to sequentially close and open, enabling a zipping sequence. Wang and Lee presented a SAPMP featuring a serpentine-shape (S-shape) microchannel enabling single source actuation for 3, 5, and 7 actuation chambers [55,111]. As the compressed air travels in the microchannels, it deflects the membrane with a phase-lag enabling peristalsis. However, when the chip size is limited the serpentine-shaped air channel fills almost immediately and significantly reduces the pumping. Further, the serpentine-shaped channel occupies a large surface on a chip. To address these issues, another concept for pneumatic-driven SAPMPs was developed where peristalsis is achieved due to actuation phase-lag enabled by the different volumes of the driver chambers [56] and an active valve [54]. In this concept, when the compressed air travels, it closes the smaller chambers first, which causes peristalsis from the smallest to the largest chamber. Using a similar phase-lag concept, vacuum has been also utilized as the actuation source for pneumatic SAPMPs [58]. Using a vacuum source not only enables peristalsis, it assists debubbling of the working fluid through the gas permeable PDMS membrane, which is highly desired in the microfluidic applications. Although SAPMPs offer various advantages, they are unidirectional by nature which could limit their applications where bidirectionality is crucial.

### 4.4 Electrostatic

Electrostatic actuation is based on the Coulomb attraction force between two plates with opposite charges. This actuation method has been used for PMPs without a transmission mechanism directly on chambers [10,73,79,112–114]. Electrostatic actuation is relatively small in footprint and overall size, with low power consumption and fast response, simple-

to-control stroke, and planar structure. However, it has small stroke and requires high operating voltage and considerations for electrolysis of polar working fluids.

Xie et al. reported an electrostatic PMP using a multilayer technology to isolate the working fluid from the electric field to minimize electrolysis [81]. Furthermore, to minimize electrolysis, an AC actuation signal was used. However, electrolysis was observed when using a polar working fluid (water), while the results of a nonpolar working fluid (ethanol) was electrolysis-free. Patrascu et al. explored comparing polar (water) and non-polar fluid (octane) in their electrostatic PMP [115]. The results demonstrate that the micropump cannot generate flow with polar fluid, while the non-polar fluid provides reliable results of  $Q_{max} = 1.38 \mu\text{L}/\text{min}$  at  $f_{Q_{max}} = 400 \text{ Hz}$ .

While electrolysis is challenging for using electrostatic mechanism with polar working fluids, this actuation method is an excellent choice for pumping non-polar fluids such as air. Electrostatic-driven PMPs have been used for gas chromatography by Najafi's group [69,116–119]. In an 18-stage configuration with 19 microvalves, extremely high flow rates and differential pressures for gas micropumps ( $Q_{max} = 4000 \mu\text{L}/\text{min}$ ,  $P_{max} = 17.5 \text{ kPa}$ ) was achieved in a tiny package size ( $S_p = 479 \text{ mm}^3$ ) and with peak-to-peak voltage ( $V_{pp}$ ) of 200 V and 57 mW power consumption [69].

#### 4.5 Thermal

Thermal actuation involves induced stress or volume change in response to applied heat. It has been used for discrete-scheme PMPs in forms of thermopneumatic (TP), phase-change (PC), shape memory alloy (SMA) [59,120–122], and hydrogel (HG) [123] actuators, typically directly on the chambers without a transmission mechanism. This actuation method creates large strokes and actuation force, with a small operating voltage and simple driving circuit, typically in a planar form factor with a small size. Since this actuation method depends on heat diffusion, it works in lower frequency ranges with large power consumption and elevates the temperature of the working fluid. Although SMA and HG were used in the literature for driving PMPs, they are not covered further here due to their minor contribution in developing PMPs.

TP actuation occurs when a fluid other than the working fluid is heated and expands without a phase-change, causing the micropump membrane to deflect and move the working fluid. Usually, the heater is a thin resistive film and air is employed as the expanding material. Several researchers investigated application of this actuation method for PMPs with experimental, lumped model, and computational approaches [40,68,124–128]. Compared to other thermal actuation methods, the TP actuation suffers from relatively larger temperature elevation in the working fluid for equal membrane deformation. Chia et al. addressed this issue by designing a side chamber for each chamber to be actuated by TP actuator with transmission of the actuation force to the chamber through a fluidic microchannel [129]. As a result of separating the actuator and the chambers the temperature elevation of the working fluid was reduced by up to 24-fold (from 70.3 to 2.9 °C).

The PC actuation method relies on volume expansion of a material due to thermal phase-change to deflect a chamber membrane and actuate the working fluid. Since the thermal

expansion occurs during the phase-change process at a fixed temperature rather than single-phase temperature elevation, this method enables actuation with lower temperature elevation in the working fluid compared to the TP method. The PC actuation method can generate extremely high actuation force depending on the phase-change material (e.g., paraffin wax [130]). Borkholder's group developed discrete-scheme phase-change PMPs for ultra-low flow ranges (10–100 nL/min) using gallium and paraffin wax actuation materials which shrink and expand during melting, respectively [30,33,131].

#### 4.6 Emerging actuation methods

Recently, new actuation methods with peristalsis capabilities were introduced. Saren et al. introduced a peristaltic like micropump with magnetic shape memory (MSM) alloy Ni-Mn-Ga [132]. An MSM element operates as a metal muscle that propels the working fluid from inlet to outlet with a continuous peristaltic-like motion due to application of an external axially rotating magnetic field. The results demonstrate pumping pressures up to 200 kPa and flow rate range of 0–2000  $\mu\text{L}/\text{min}$  with 50–150 nL resolution per pumping cycle. Wu et al. developed a numerical model for a PMP based on the principle of using an external magnetic field to actuate a magnetorheological elastomer (MRE) tube [133]. The tube was made of silicone, filled with silica-coated carbonyl iron particles as a typical MRE with a well-characterized magnetization curve. The model consisted of several elements of MRE tubings and electromagnets connected in series to create peristalsis. Yamatsuta et al. reported a PMP built around a micro peristaltic tubing powered by a light-responsive *Drosophila melanogaster* larvae muscle for a potential application in integrated tissue-engineered soft robots [134]. Peristalsis was obtained by changing the speed of the propagating blue light stimulator on tubular structures (400  $\mu\text{m}$  ID, 750  $\mu\text{m}$  OD) dissected from larvae, causing displacement on the surface of the contractile muscle tissues. The micropump generated flow rates up to 0.72  $\mu\text{L}/\text{min}$  with optimal wave propagation speed of 400  $\mu\text{m}/\text{s}$ . Bandopadhyay et al. analytically explored an electroosmosis-modulated actuation mechanism demonstrating potential for creating PMP for LOC applications [135].

#### 4.7 Summary

Various actuation methods for driving PMPs were described from the literature along with their advantages and disadvantages, and examples of reported research efforts to improve them for PMPs. Depending on the application of the PMP, a designer needs to consider the critical characteristics of each actuation method such as size, fabrication complexity, operating frequency, power consumption, and compatibility to the specific environment. Table 3 qualitatively compares these actuation methods with listing their typical advantages and disadvantages in the current designs for common applications in microfluidics.

## 5 Evaluation and discussion

### 5.1 Advantages and disadvantages of PMPs

PMPs are relatively simple in structure, suitable for miniaturization, and straightforward to fabricate since they have similar chamber configurations, enabling simple integration on a single substrate. PMPs offer post-fabrication tuning of the flow rate range by changing channels with different inner diameters in modular design configurations (e.g., [71]). PMPs

are reliable, enduring, tolerant to bubbles, and capable of self-priming and handling viscous working fluids. PMPs provide continuous, clean, and clogless flow path due to the absence of inline valves which is critical in small fluid channels, and especially to keep the samples free of contamination, intact, and unclogged. Due to these characteristics, PMPs have been used in many applications in biomedical, chemical and nutrition, and pharmaceutical industries. Additionally, PMPs operate gently, potentially on multiple fluid conduits, which enables them to handle sensitive biological media or suspensions, and multiple samples at the same time. Bi-directional and pulsatile flow capacities of PMPs enable them to serve in several LOC applications, where circulating flow in microfluidic channels or mimicking pulsatile *in vivo* fluid mechanical environments are required. PMPs are typically planar, an advantageous feature for LOC and implantable drug delivery applications, where on-chip integration to other elements, and minimizing device thickness are crucial. Although PMPs have several benefits, they suffer from mechanical wear, especially the continuous-scheme PMPs. Further, low efficiency is observed in PMPs due to the absence of check valves. Another drawback of PMPs is the complexity of independent synchronized actuation of multiple chambers, which is more common in the discrete-scheme PMPs.

## 5.2 Comparison of different PMPs

In this section, we review reported PMPs with major contributions in developing PMPs since their emergence in 1990. Various PMPs have been developed with different actuation and rectification methods, for several applications. Several characteristics are considered here, including  $Q_{max}$  and  $P_{max}$  which are two key merits of a micropump. Since many PMPs have been used for size-constrained applications, such as drug delivery and LOC, the overall package size ( $S_p$ ) and the package surface area on the chip ( $A_p$ ) are also considered. Where  $S_p$  and  $A_p$  are not reported, they are estimated from provided images and scales. We attempted to include pump structure (e.g., microchannels) and actuators (e.g., motor, piezoelectric discs) for estimation of  $S_p$ , while power supplies and driving circuits are excluded since they are not usually reported. For pneumatic PMPs, the  $S_p$  excludes compressed air or vacuum source, solenoid valves and their driving circuits.  $A_p$ , however, just considers the footprint of a PMP on a fluidic chip, which is a critical parameter for integration of a PMP to other elements in a microfluidic chip, especially for LOC systems.  $V_{pp}$ ,  $f$ , and  $PW$  at the reported  $Q_{max}$  ( $V_{Q_{max}}$ ,  $f_{Q_{max}}$ ,  $PW_{Q_{max}}$ ) are also considered here since they impact potential application of the PMPs and driving circuit complexity and size. When  $PW$  is not explicitly reported, we attempted to estimate based on other reported data (i.e., voltage, current, and resistance).

Key features and measured performance characteristics of different PMPs are summarized in Table 4. In this table PMPs are arranged based on their actuation methods, while other characteristics of them such as transmission mechanism, actuation scheme, fluidic channel configuration, and self-reported applications are provided. For all the PMPs, the working fluid is liquid (usually DI water) except for PMPs for gas chromatography [10,69].

Figure 3 quantitatively compares different PMPs in terms of actuation method (Figure 3A–H) and scheme (Figure 3I) for a better insight into advantages and disadvantages of each. Motor and thermal -driven PMPs perform with lower actuation voltages and frequencies

relative to piezoelectric and electrostatic PMPs that typically operate with an order of magnitude larger operating voltages and frequencies (Figure 3A and B). Thermally-driven PMPs consume up to an order of magnitude more power compared to other methods (Figure 3C). Electrostatic and pneumatic PMPs can provide at least an order of magnitude smaller package sizes and on-chip footprint, while thermally-driven PMPs can also be relatively small in package size and footprint (Figure 3D and E). Figure 3F and G show that electrostatic and pneumatic PMPs yield the largest flow rate per package size (self-pumping frequency,  $f_{sp} = Q_{max} / S_p$  [1]) and flow rate per footprint (self-pumping velocity,  $V_{sp} = Q_{max} / A_p$ ). Electrostatic PMPs also provide the largest power flow rate efficiency ( $\zeta = Q/PW$ ) among others, and thermal PMPs have approximately two orders of magnitude less flow rate per consumed power relative to other actuation methods (Figure 3H). Finally, a comparison between discrete and continuous-scheme PMPs demonstrate the capability of continuous-scheme PMPs to provide at least an order of magnitude larger  $P_{max}$  than the discrete-scheme ones (Figure 3I).

Figure 4 compares PMPs based on four different metrics:  $Q_{max}$ ,  $S_p$ ,  $P_{max}$ , and actuation method. The  $Q_{max}$  is plotted along the ordinate, and the reported or estimated  $S_p$  is along the abscissa. As depicted in the legend, the actuation methods are distinguished by color, while the data point size represents the  $P_{max}$  range.

A few observations can be made. A direct correlation between  $Q_{max}$  and  $S_p$  can be observed. The 18-stage electrostatic micropump with air as working fluid reported by Kim et al. has the highest  $f_{sp}$  ( $8.4 \text{ min}^{-1}$ ) and maximum flow rate ( $Q_{max} = 4000 \text{ }\mu\text{L}/\text{min}$ ) [69]. The pneumatic-driven PMP reported by Cui et al. provides the largest  $f_{sp}$  among PMPs working with liquid ( $5.6 \text{ min}^{-1}$ ), with  $Q_{max} = 600 \text{ }\mu\text{L}/\text{min}$  [58]. The pneumatic PMP reported by Unger et al. minimized the package as small as  $2 \text{ mm}^3$  with maximum flow rate of  $0.14 \text{ }\mu\text{L}/\text{min}$  [110].

Motor-driven PMPs cover a large range of flow rates while working with low voltage and generating higher pressures, due to their actuation method and flexibility to couple to different transmission mechanisms. Due to these advantages motor-driven PMPs have gained particular attention and are now available commercially (e.g. iPRECIO® PMPs). However, the smallest motor-driven PMP (iPRECIO® SMP-310R [86]) is  $\sim 2000 \text{ mm}^3$  in size (excluding the reservoir and the battery) which limits applications for extremely size-constrained applications such as implantation in small rodents. The bottleneck of size reduction for motor-driven devices is the size of motors. Reducing the size of reliable and well-controlled motors can substantially assist further miniaturization of these PMPs with precision control over flow rate enabling their applications in even further applications.

Piezoelectric-driven PMPs were also widely used in the literature, since they are capable of generating higher flow rates while being able to generate high pressures. However, high voltage and complicated driving circuits remain a challenge in these micropumps, especially for drug delivery applications. The sol-gel PZT PMP reported by Cazorla et al. was able to reduce the driving voltage to 24 V while keeping high generated pressure, but at the cost of maximum flow rate ( $Q_{max} = 3.5 \text{ }\mu\text{L}/\text{min}$ ) [28]. Further research on miniaturization of piezoelectric PMPs, while maintaining low operating voltage can broaden their application

in various fields, including drug delivery. Although pneumatic PMPs were miniaturized as small as  $2 \text{ mm}^3$  [110], it is worth noting that the package size excludes the solenoid valves and pneumatic pressure/vacuum sources which are usually from a compressed air line or a vacuum pump. Further research on minimizing the pressure/vacuum sources and control valves may be warranted.

Thermal PMPs have been used to generate ultra-low flow rates ( $\sim 100 \text{ nL/min}$ ) with a relatively smaller package size (tens to hundreds  $\text{mm}^3$ ). Although these pumps suffer from inherent larger  $PW$ , they can be further miniaturized and be used in applications with smaller flow rates where  $S_p$  has higher priority than  $PW$ , such as subcutaneous implantable drug delivery systems with transdermal power (e.g., induction). Electrostatic PMPs offer excellent miniaturization capabilities and power flow rate efficiency, however, the high operating voltage limits applications due to electrolysis with polar working fluids. Further research on clever ways to reduce the operating voltage such as change in the chamber geometry with reducing  $V_{st}$  and increasing  $f$  (to maintain  $Q$ ) may be warranted. Separation of actuators and chambers using a transmission mechanism can address the electrolysis issue for these PMPs.

## 6 Conclusions and future outlook

The brief survey given in this paper reviews a variety of PMP concepts, key parameters affecting pump operation, and actuation methods since their emergence in 1990. The peristalsis concept was explained in depth, defined as a rectification method in mechanical micropumps, and distinguishing it from other rectification methods. Various parameters that substantially impact the operation of PMPs were discussed, including operating frequency, peristalsis sequence, and the number of chambers. Several research efforts in the literature to implement PMPs with various actuation methods were reviewed.

Creating the actuation sequence for peristalsis is a source of complexity for discrete-scheme PMPs; in some cases it causes a larger package size. However, researchers attempted to address this issue by developing SAPMPs where a single actuator generates the actuation force and a delaying transmission mechanism generates peristalsis [54–56]. Researchers also developed  $PtP$  convertor mechanisms that enable using actuators with perpendicular motion relative to the flow channel, creating continuous-scheme pumping [52,59,60]. In both these mechanisms one actuator drives the micropump and the peristalsis is embedded into the structure of the device to avoid controlling the sequence with synchronized signals. Using a single actuator with a mechanism to create peristalsis for other actuation methods expands the capabilities and applications of PMPs, due to different characteristics of each actuation method (see section 4). Additionally, PMPs with one actuator potentially reduce the overall package size, a crucial feature for size-constrained applications.

Although the significant parameters in peristalsis (e.g., operating sequence, number of chambers, etc.) have been studied subjectively in the literature, a generic model for optimization of these factors would be immensely useful for researchers as a design rule for developing new devices. For such a model, the parameters discussed in this paper (section 3) should be taken into consideration, along with the limitations and advantages



of each actuation method presented in section 4. Optimized devices, considering all factors mentioned above, can compensate for the lack of check valves in the system and improve the efficiency of PMPs.

The most common applications of PMPs are LOC and drug delivery (See Table 4). For these applications, increasing self-pumping frequency ( $f_{sp} = Q_{max} / S_p$ ) is necessary and remains a challenge. For drug delivery applications miniaturization is essential due to the size-limited nature of the application. Approaches for miniaturization include using the SAPMP or *PtP* convertor concepts to reduce the size of mechanical and control electronics components, developing smaller motors, using miniaturized pneumatic sources and controllers, etc. Integrability of the PMPs to the driving circuit, power supply (e.g. battery for most PMPs, and compressed air for pneumatic PMPs), and reservoirs (e.g., [136,137]) is another factor to consider. For LOC applications, integrability enables a self-contained pumping mechanism that is useful, especially for applications that require incubators, independent of external connections (e.g. wires, pneumatic tubes, etc.). For drug delivery applications the self-contained platform is essential due to limitations for accessing external connections. To improve functionality of PMPs, embedding monitoring mechanisms such as flow sensors assist feedback control in adjusting the flow rate by perhaps changing the operating frequency as the most accessible/simple post-fabrication control mechanism. For drug delivery applications, such a mechanism enables informing the user and health care provider of the status and performance of the pump providing confidence the system is delivering the correct dosage.

## Supplementary Material

Refer to Web version on PubMed Central for supplementary material.

## References

- [1]. Laser DJ, Santiago JG, A review of micropumps, *J. Micromechanics Microengineering* 14 (2004) R35–R64. 10.1088/0960-1317/14/6/R01.
- [2]. Shoji S, Esashi M, Microflow devices and systems, *J. Micromechanics Microengineering* 4 (1994) 157–171. 10.1088/0960-1317/4/4/001.
- [3]. Nguyen N-T, Huang X, Chuan TK, MEMS-Micropumps: A Review, *J. Fluids Eng* 124 (2002) 384. 10.1115/1.1459075.
- [4]. Leu TS, Gong DC, Pan D, Numerical and experimental studies of phase difference effects on flow rate of peristaltic micro-pumps with pumping chambers in series configurations, *Microsyst. Technol* 23 (2017) 329–341. 10.1007/s00542-015-2529-0.
- [5]. Iverson BD, Garimella SV, Recent advances in microscale pumping technologies: A review and evaluation, *Microfluid. Nanofluidics* 5 (2008) 145–174. 10.1007/s10404-008-0266-8.
- [6]. Nisar A, Afzulpurkar N, Mahaisavariya B, Tuantranont A, MEMS-based micropumps in drug delivery and biomedical applications, *Sensors Actuators, B Chem.* 130 (2008) 917–942. 10.1016/j.snb.2007.10.064.
- [7]. Smits JG, Piezoelectric micropump with three valves working peristaltically, *Sensors Actuators A Phys.* 21 (1990) 203–206. 10.1016/0924-4247(90)85039-7.
- [8]. Yang S-Y, Hsiung S-K, Hung Y-C, Chang C-M, Liao T-L, Lee G-B, A cell counting/sorting system incorporated with a microfabricated flow cytometer chip, *Meas. Sci. Technol* 17 (2006) 2001. 10.1088/0957-0233/17/7/045.

- [9]. Sabourin D, Skaft-Pedersen P, S e MJ, Hemmingsen M, Alberti M, Coman V, Petersen J, Emn us J, Kutter JP, Snakenborg D, J rgensen F, Clausen C, Holmstr m K, Dufva M, The MainSTREAM Component Platform: A Holistic Approach to Microfluidic System Design, *J. Lab. Autom* 18 (2013) 212–228. 10.1177/2211068212461445. [PubMed: 23015520]
- [10]. Lee I, Hong P, Cho C, Lee B, Chun K, Kim B, Four-electrode micropump with peristaltic motion, *Sensors Actuators, A Phys.* 245 (2016) 19–25. 10.1016/j.sna.2016.04.010.
- [11]. Nightingale A, Evans GWH, Xu P, Kim BJ, Hassan S, Niu X, Phased peristaltic micropumping for continuous sampling and hardcoded droplet generation, *Lab Chip.* (2017). 10.1039/C6LC01479H.
- [12]. Cheng Y, Wang Y, Ma Z, Wang W, Ye X, A bubble- and clogging-free microfluidic particle separation platform with multi-filtration, *Lab Chip.* 16 (2016) 4517–4526. 10.1039/C6LC01113F. [PubMed: 27792227]
- [13]. Didar TF, Li K, Tabrizian M, Veres T, High throughput multilayer microfluidic particle separation platform using embedded thermoplastic-based micropumping, *Lab Chip.* 13 (2013) 2615–2622. 10.1039/c3lc50181g. [PubMed: 23640083]
- [14]. Cheng Y, Ye X, Ma Z, Xie S, Wang W, High-throughput and clogging-free microfluidic filtration platform for on-chip cell separation from undiluted whole blood, *Biomicrofluidics.* 10 (2016) 014118. 10.1063/1.4941985. [PubMed: 26909124]
- [15]. Sasaki N, Shinjo M, Hirakawa S, Nishinaka M, Tanaka Y, Mawatari K, Kitamori T, Sato K, A palm-top-sized microfluidic cell culture system driven by a miniaturized infusion pump, *Electrophoresis.* 33 (2012) 1729–1735. 10.1002/elps.201100691. [PubMed: 22740461]
- [16]. Wagner I, Materne EM, Brincker S, S bbier U, Fr drich C, Busek M, Sonntag F, Sakharov DA, Trushkin EV, Tonevitsky AG, Lauster R, Marx U, A dynamic multi-organ-chip for long-term cultivation and substance testing proven by 3D human liver and skin tissue co-culture, *Lab Chip.* 13 (2013) 3538–3547. 10.1039/c3lc50234a. [PubMed: 23648632]
- [17]. Futai N, Gu W, Song JW, Takayama S, Handheld recirculation system and customized media for microfluidic cell culture, *Lab Chip.* 6 (2006) 149–154. 10.1039/b510901a. [PubMed: 16372083]
- [18]. Hsu YC, Lin SJ, Hou CC, Development of peristaltic antithrombogenic micropumps for in vitro and ex vivo blood transportation tests, *Microsyst. Technol* 14 (2008) 31–41. 10.1007/s00542-007-0405-2.
- [19]. Du M, Ma Z, Ye X, Zhou Z, On-chip fast mixing by a rotary peristaltic micropump with a single structural layer, *Sci. China Technol. Sci* 56 (2013) 1047–1054. 10.1007/s11431-013-5140-6.
- [20]. Weng CH, Yeh WM, Ho KC, Bin Lee G, A microfluidic system utilizing molecularly imprinted polymer films for amperometric detection of morphine, *Sensors Actuators, B Chem.* 121 (2007) 576–582. 10.1016/j.snb.2006.04.111.
- [21]. Bar-Cohen Y, Chang Z, Piezoelectrically actuated miniature peristaltic pump, in: *Smart Struct. Mater. 2000 Act. Mater. Behav. Mech.*, 2000: pp. 669–676.
- [22]. Wang CH, Bin Lee G, Automatic bio-sampling chips integrated with micro-pumps and micro-valves for disease detection, *Biosens. Bioelectron* 21 (2005) 419–425. 10.1016/j.bios.2004.11.004. [PubMed: 16076430]
- [23]. Doll A, Heinrichs M, Goldschmidtboeing F, Schrag HJ, Hopt UT, Woias P, A high performance bidirectional micropump for a novel artificial sphincter system, *Sensors Actuators, A Phys.* 130–131 (2006) 445–453. 10.1016/j.sna.2005.10.018.
- [24]. Sun Y, Quyen TL, Hung TQ, Chin WH, Wolff A, Bang DD, A lab-on-a-chip system with integrated sample preparation and loop-mediated isothermal amplification for rapid and quantitative detection of *Salmonella* spp. in food samples, *Lab Chip.* 15 (2015) 1898–1904. 10.1039/C4LC01459F. [PubMed: 25715949]
- [25]. Skaft-Pedersen P, Sabourin D, Dufva M, Snakenborg D, Multi-channel peristaltic pump for microfluidic applications featuring monolithic PDMS inlay, *Lab Chip.* 9 (2009) 3003–3006. 10.1039/b906156h. [PubMed: 19789757]
- [26]. Ma T, Sun S, Li B, Chu J, Piezoelectric peristaltic micropump integrated on a microfluidic chip, *Sensors Actuators, A Phys.* 292 (2019) 90–96. 10.1016/j.sna.2019.04.005.

- [27]. Cao L, Mantell S, Polla D, Design and simulation of an implantable medical drug delivery system using microelectromechanical systems technology, *Sensors Actuators, A Phys.* 94 (2001) 117–125. 10.1016/S0924-4247(01)00710-5.
- [28]. Cazorla PH, Fuchs O, Cochet M, Maubert S, Le Rhun G, Fouillet Y, Defay E, A low voltage silicon micro-pump based on piezoelectric thin films, *Sensors Actuators, A Phys.* 250 (2016) 35–39. 10.1016/j.sna.2016.09.012.
- [29]. Speed JS, Hyndman KA, In vivo organ specific drug delivery with implantable peristaltic pumps, *Sci. Rep* 6 (2016) 1–7. 10.1038/srep26251. [PubMed: 28442746]
- [30]. Forouzandeh F, Alfadhel A, Zhu X, Walton JP, Cormier DR, Frisina RD, Borkholder DA, A wirelessly controlled fully implantable microsystem for nano-liter resolution inner ear drug delivery, in: 18th Solid-State Sensors, Actuators, Microsystems Work. Hilt. Head Island, SC, USA, 2018: pp. 38–41. 10.31438/trf.hh2018.11.
- [31]. Forouzandeh F, *Implantable Microsystem Technologies For Nanoliter-Resolution Inner Ear Drug Delivery*, 2019.
- [32]. Forouzandeh F, Zhu X, Ahamed NN, Walton JP, Frisina RD, Borkholder DA, A modular microreservoir for active implantable drug delivery, *BioRxiv.* (2019) 762716. 10.1101/762716.
- [33]. Forouzandeh F, Zhu X, Alfadhel A, Ding B, Walton JP, Cormier D, Frisina RD, Borkholder DA, A nanoliter resolution implantable micropump for murine inner ear drug delivery, *J. Control. Release* 298 (2019) 27–37. 10.1016/j.jconrel.2019.01.032. [PubMed: 30690105]
- [34]. Salt A, Hartsock J, Gill R, Smyth D, Kirk J, Verhoeven K, Perilymph pharmacokinetics of marker applied through a cochlear implant in guinea pigs, *PLoS One.* 12 (2017) e0183374. 10.1371/journal.pone.0183374. [PubMed: 28817653]
- [35]. Forouzandeh F, Borkholder DA, *Microtechnologies for inner ear drug delivery*, *Curr. Opin. Otolaryngol. Head Neck Surg* (2020). 10.1097/moo.0000000000000648.
- [36]. Geipel A, Goldschmidtboeing F, Jantschke P, Esser N, Massing U, Woias P, Design of an implantable active microport system for patient specific drug release, *Biomed. Microdevices* 10 (2008) 469–478. 10.1007/s10544-007-9147-2. [PubMed: 18483865]
- [37]. Vinayakumar KB, Nadiger G, Shetty VR, Dinesh NS, Nayak MM, Rajanna K, Packaged peristaltic micropump for controlled drug delivery application, *Rev. Sci. Instrum* 88 (2017) 015102. 10.1063/1.4973513. [PubMed: 28147679]
- [38]. Woias P, Micropumps—past, progress and future prospects, *Sensors Actuators B Chem.* (2005). <http://www.sciencedirect.com/science/article/pii/S092540050400108X> (accessed August 18, 2015).
- [39]. Au AK, Lai H, Utela BR, Folch A, Microvalves and micropumps for BioMEMS, 2011. 10.3390/mi2020179.
- [40]. Grosjean C, Tai Y, A thermopneumatic peristaltic micropump, *Proc. Transducer* (1999). [https://scholar.google.com/scholar?q=A+thermopneumatic+peristaltic+micropump&btnG=&hl=en&as\\_sdt=0%2C33](https://scholar.google.com/scholar?q=A+thermopneumatic+peristaltic+micropump&btnG=&hl=en&as_sdt=0%2C33) (accessed March 6, 2017).
- [41]. Xie J, Shih J, Integrated Parylene Electrostatic peristaltic pump, (2003) 0–3.
- [42]. Goldschmidtboeing F, Doll A, Heinrichs M, Woias P, Schrag H-J, Hopt UT, A generic analytical model for micro-diaphragm pumps with active valves, *J. Micromechanics Microengineering* 15 (2005) 673–683. 10.1088/0960-1317/15/4/001.
- [43]. Bu MQ, Tracy M, Ensell G, Wilkinson JS, Evans AGR, Design and theoretical evaluation of a novel microfluidic device to be used for PCR, *J. Micromechanics Microengineering* 13 (2003) S125–S130.
- [44]. Johnson DG, Frisina RD, Borkholder DA, In-Plane Biocompatible Microfluidic Interconnects for Implantable Microsystems, *IEEE Trans. Biomed. Eng* 58 (2011) 943–948. 10.1109/TBME.2010.2098031. [PubMed: 21147591]
- [45]. Chen C, Shih S, Hsu C, Fabrication of a Peristaltic Micropump with UV Curable Adhesive, *Proc. 3rd Int. Conf. Intell. Technol. Eng. Syst* 293 (2016) 119–125. 10.1007/978-3-319-04573-3.
- [46]. Chiou C-H, Yeh T-Y, Lin J-L, Deformation Analysis of a Pneumatically-Activated Polydimethylsiloxane (PDMS) Membrane and Potential Micro-Pump Applications, *Micromachines.* 6 (2015) 216–229. 10.3390/mi6020216.

- [47]. Shaegh SAM, Wang Z, Ng SH, Wu R, Nguyen HT, Chan LCZ, Toh AGG, Wang Z, Plug-and-play microvalve and micropump for rapid integration with microfluidic chips, *Microfluid. Nanofluidics* 19 (2015) 557–564. 10.1007/s10404-015-1582-4.
- [48]. Zhang W, Eitel RE, An Integrated Multilayer Ceramic Piezoelectric Micropump for Microfluidic Systems, *J. Intell. Mater. Syst. Struct* 24 (2013) 1637–1646. 10.1177/1045389X13483023.
- [49]. Kant R, Singh H, Nayak M, Bhattacharya S, Optimization of design and characterization of a novel micropumping system with peristaltic motion, *Microsyst. Technol* 19 (2013) 563–575. 10.1007/s00542-012-1658-y.
- [50]. Nguyen NT, Huang X, Miniature valveless pumps based on printed circuit board technique, *Sensors Actuators, A Phys.* 88 (2001) 104–111. 10.1016/S0924-4247(00)00500-8.
- [51]. Berg JM, Anderson R, Anaya M, Lahlouh B, Holtz M, Dallas T, A two-stage discrete peristaltic micropump, *Sensors Actuators, A Phys.* 104 (2003) 6–10. 10.1016/S0924-4247(02)00434-X.
- [52]. Pe ar B, Križaj D, Vrta nik D, Resnik D, Dolžan T, Možek M, Piezoelectric peristaltic micropump with a single actuator, *J. Micromechanics Microengineering* 24 (2014) 105010. 10.1088/0960-1317/24/10/105010.
- [53]. Geipel A, Doll A, Jantscheff P, Esser N, Massing U, Woias P, Goldschmidtboeing F, A novel two-stage backpressure-independent micropump: modeling and characterization, *J. Micromechanics Microengineering* 17 (2007) 949–959. 10.1088/0960-1317/17/5/015.
- [54]. Huang C-W, Huang S-B, Lee G-B, Pneumatic micropumps with serially connected actuation chambers, *J. Micromechanics Microengineering* 16 (2006) 2265–2272. 10.1088/0960-1317/16/11/003.
- [55]. Wang C-H, Lee G-B, Pneumatically driven peristaltic micropumps utilizing serpentine-shape channels, *J. Micromechanics Microengineering* 16 (2006) 341–348. 10.1088/0960-1317/16/2/019.
- [56]. Lai H, Folch A, Design and dynamic characterization of “single-stroke” peristaltic PDMS micropumps, *Lab Chip*. 11 (2011) 336–342. 10.1039/c0lc00023j. [PubMed: 20957288]
- [57]. Shao J, Wu L, Wu J, Zheng Y, Zhao H, Jin Q, Zhao J, Integrated microfluidic chip for endothelial cells culture and analysis exposed to a pulsatile and oscillatory shear stress, *Lab Chip*. 9 (2009) 3118–3125. 10.1039/b909312e. [PubMed: 19823728]
- [58]. Cui J, Pan T, A vacuum-driven peristaltic micropump with valved actuation chambers, *J Micromech Microeng.* 21 (2011) 065034. 10.1088/0960-1317/21/6/065034.
- [59]. Shkolnikov V, Ramunas J, Santiago JG, A self-priming, roller-free, miniature, peristaltic pump operable with a single, reciprocating actuator, *Sensors Actuators, A Phys.* 160 (2010) 141–146. 10.1016/j.sna.2010.04.018.
- [60]. Nakahara K, Yamamoto M, Okayama Y, Yoshimura K, Fukagata K, Miki N, A peristaltic micropump using traveling waves on a polymer membrane, *J. Micromechanics Microengineering* 23 (2013) 085024. 10.1088/0960-1317/23/8/085024.
- [61]. Pe ar B, Vrta nik D, Resnik D, Možek M, Aljan i U, Dolžan T, Amon S, Križaj D, A strip-type microthrottle pump: Modeling, design and fabrication, *Sensors (Switzerland)*. 13 (2013) 3092–3108. 10.3390/s130303092.
- [62]. Beckers G, Dehez B, Design and modeling of a quasi-static peristaltic piezoelectric micropump, *2013 Int. Conf. Electr. Mach. Syst. ICEMS 2013* (2013) 1301–1306. 10.1109/ICEMS.2013.6713258.
- [63]. Tsui YY, Chang TC, A novel peristaltic micropump with low compression ratios, *Int. J. Numer. Methods Fluids* 69 (2012) 1363–1376. 10.1002/flid.2644.
- [64]. Hsu YC, Le NB, Equivalent electrical network for performance characterization of piezoelectric peristaltic micropump, *Microfluid. Nanofluidics* 7 (2009) 237–248. 10.1007/s10404-008-0380-7.
- [65]. Busek M, Nötzel M, Polk C, Sonntag F, Characterization and simulation of peristaltic micropumps, *J. Sensors Sens. Syst* 2 (2013) 165–169. 10.5194/jsss-2-165-2013.
- [66]. Na S, Ridgeway S, Cao L, Theoretical and experimental study of fluid behavior of a peristaltic micropump, *Bienn. Univ. Microelectron. Symp. - Proc* (2003) 312–316. 10.1109/ugim.2003.1225751.

- [67]. Lin Q, Yang B, Xie J, Tai Y-C, Dynamic simulation of a peristaltic micropump considering coupled fluid flow and structural motion, *J. Micromechanics Microengineering* 17 (2006) 220–228. 10.1088/0960-1317/17/2/006.
- [68]. Yang Y-J, Liao H-H, Development and characterization of thermopneumatic peristaltic micropumps, *J. Micromechanics Microengineering* 19 (2009) 025003. 10.1088/0960-1317/19/2/025003.
- [69]. Kim H, Astle AA, Najafi K, Bernal LP, Washabaugh PD, An integrated electrostatic peristaltic 18-stage gas micropump with active microvalves, *J. Microelectromechanical Syst* 24 (2015) 192–206. 10.1109/JMEMS.2014.2327096.
- [70]. Lee DS, Ko JS, Kim YT, Bidirectional pumping properties of a peristaltic piezoelectric micropump with simple design and chemical resistance, *Thin Solid Films*. 468 (2004) 285–290. 10.1016/j.tsf.2004.05.014.
- [71]. Koch C, Remcho V, Ingle J, PDMS and tubing-based peristaltic micropumps with direct actuation, *Sensors Actuators, B Chem*. 135 (2009) 664–670. 10.1016/j.snb.2008.10.019.
- [72]. Yobas L, Tang KC, Yong SE, Kye-Zheng Ong E, A disposable planar peristaltic pump for lab-on-a-chip, *Lab Chip*. 8 (2008) 660–662. 10.1039/b720024b. [PubMed: 18432333]
- [73]. Lee KS, Kim B, Shannon MA, An electrostatically driven valve-less peristaltic micropump with a stepwise chamber, *Sensors Actuators, A Phys*. 187 (2012) 183–189. 10.1016/j.sna.2012.08.040.
- [74]. Jeong OC, Konishi S, Fabrication of a peristaltic micro pump with novel cascaded actuators, *J. Micromechanics Microengineering* 18 (2008) 025022. 10.1088/0960-1317/18/2/025022.
- [75]. Jang LS, Kan WH, Peristaltic piezoelectric micropump system for biomedical applications, *Biomed. Microdevices* 9 (2007) 619–626. 10.1007/s10544-007-9075-1. [PubMed: 17505886]
- [76]. Chao CS, Huang PC, Chen MK, Jang LS, Design and analysis of charge-recovery driving circuits for portable peristaltic micropumps with piezoelectric actuators, *Sensors Actuators, A Phys*. 168 (2011) 313–319. 10.1016/j.sna.2011.04.027.
- [77]. Jang LS, Yu YC, Peristaltic micropump system with piezoelectric actuators, *Microsyst. Technol* 14 (2008) 241–248. 10.1007/s00542-007-0428-8.
- [78]. Jang LS, Shu K, Yu YC, Li YJ, Chen CH, Effect of actuation sequence on flow rates of peristaltic micropumps with PZT actuators, *Biomed. Microdevices* 11 (2009) 173–181. 10.1007/s10544-008-9222-3. [PubMed: 18821016]
- [79]. Lee KS, Kim B, a Shannon M, Development of a peristaltic gas micropump with a single chamber and multiple electrodes, *J. Micromechanics Microengineering* 23 (2013) 095006. 10.1088/0960-1317/23/9/095006.
- [80]. Graf NJ, Bowser MT, A soft-polymer piezoelectric bimorph cantilever-actuated peristaltic micropump., *Lab Chip*. 8 (2008) 1664–70. 10.1039/b805252b. [PubMed: 18813388]
- [81]. Xie J, Shih J, Lin Q, Yang B, Tai Y-C, Surface micromachined electrostatically actuated micro peristaltic pump., *Lab Chip*. 4 (2004) 495–501. 10.1039/b403906h. [PubMed: 15472734]
- [82]. Loth A, Forster R, Disposable high pressure peristaltic micro pump for standalone and on-chip applications, in: 2016 IEEE 11th Annu. Int. Conf. Nano/Micro Eng. Mol. Syst. NEMS 2016, 2016: pp. 29–33. 10.1109/NEMS.2016.7758193.
- [83]. Zhang X, Chen Z, Huang Y, A valve-less microfluidic peristaltic pumping method, *Biomicrofluidics*. 9 (2015) 1–8. 10.1063/1.4907982.
- [84]. Xiang J, Cai Z, Zhang Y, Wang W, A micro-cam actuated linear peristaltic pump for microfluidic applications, *Sensors Actuators, A Phys*. 251 (2016) 20–25. 10.1016/j.sna.2016.09.008.
- [85]. Tamadon I, Simoni V, Iacovacci V, Vistoli F, Ricotti L, Menciasci A, Miniaturized peristaltic rotary pump for non-continuous drug dosing, *Proc. Annu. Int. Conf. IEEE Eng. Med. Biol. Soc. EMBS* (2019) 5522–5526. 10.1109/EMBC.2019.8857811.
- [86]. IPRECIO SMP-310R, (n.d.). <https://www.iprecio.com/products/tabid/245/Default.aspx> (accessed July 3, 2020).
- [87]. Tan T, Watts SW, Davis RP, Drug delivery: Enabling technology for drug discovery and development. iPRECIO® Micro Infusion Pump: programmable, refillable, and implantable, *Front. Pharmacol JUL* (2011) 44. 10.3389/fphar.2011.00044.

- [88]. Abe C, Tashiro T, Tanaka K, Ogihara R, Morita H, A novel type of implantable and programmable infusion pump for small laboratory animals, *J. Pharmacol. Toxicol. Methods* 59 (2009) 7–12. 10.1016/j.vascn.2008.09.002. [PubMed: 18852057]
- [89]. Pan T, Kai E, Stay M, Barocas V, Ziaie B, A magnetically driven PDMS peristaltic micropump, *Annu. Int. Conf. IEEE Eng. Med. Biol. - Proc.* 26 IV (2004) 2639–2642. 10.1109/iembs.2004.1403757.
- [90]. Kai E, Pan T, Ziaie B, A robust low-cost PDMS peristaltic micropump, 2 (2004) 270–273.
- [91]. Yu H, Ye W, Zhang W, Yue Z, Liu G, Design, fabrication, and characterization of a valveless magnetic travelling-wave micropump, *J. Micromechanics Microengineering* 25 (2015). 10.1088/0960-1317/25/6/065019.
- [92]. Shen M, Dovat L, Gijs MAM, Magnetic active-valve micropump actuated by a rotating magnetic assembly, *Sensors Actuators, B Chem.* 154 (2011) 52–58. 10.1016/j.snb.2009.10.033.
- [93]. Du M, Ye X, Wu K, Zhou Z, A Peristaltic Micro Pump Driven by a Rotating Motor with Magnetically Attracted Steel Balls, *Sensors.* 9 (2009) 2611–2620. 10.3390/s90402611. [PubMed: 22574035]
- [94]. Kim EG, Sim WC, Oh J, Choi B, A continuous peristaltic micropump using magnetic fluid, 2nd *Annu. Int. IEEE-EMBS Spec. Top. Conf. Microtechnologies Med. Biol. - Proc* (2002) 509–513. 10.1109/MMB.2002.1002392.
- [95]. Kim E, Oh J, Choi B, A study on the development of a continuous peristaltic micropump using magnetic fluids, *Sensors Actuators A. Phys* 128 (2006) 43–51. 10.1016/j.sna.2006.01.021.
- [96]. Hatch A, Kamholz AE, Holman G, Yager P, Böhringer KF, A ferrofluidic magnetic micropump, *J. Microelectromechanical Syst* 10 (2001) 215–221. 10.1109/84.925748.
- [97]. Husband B, Bu M, Apostolopoulos V, Melvin T, Evans AGR, Novel actuation of an integrated peristaltic micropump, *Microelectron. Eng* 73–74 (2004) 858–863. 10.1016/j.mee.2004.03.065.
- [98]. Husband B, Bu M, Evans A G.R., Melvin T, Investigation for the operation of an integrated peristaltic micropump, *J. Micromechanics Microengineering* 14 (2004) S64–S69. 10.1088/0960-1317/14/9/011.
- [99]. Lee DS, Yoon HC, Ko JS, Fabrication and characterization of a bidirectional valveless peristaltic micropump and its application to a flow-type immunoanalysis, *Sensors Actuators, B Chem.* 103 (2004) 409–415. 10.1016/j.snb.2004.04.081.
- [100]. Geipel A, Doll A, Goldschmidtboing F, Jantschke P, Esser N, Massing U, Woias P, Pressure-Independent Micropump with Piezoelectric Valves for Low Flow Drug Delivery Systems, 19th *IEEE Int. Conf. Micro Electro Mech. Syst* (2006) 786–789. 10.1109/MEMSYS.2006.1627917.
- [101]. Gu W, Zhu X, Futai N, Cho BS, Takayama S, Computerized microfluidic cell culture using elastomeric channels and Braille displays, *Proc. Natl. Acad. Sci. U. S. A* 101 (2004) 15861–15866. 10.1073/pnas.0404353101. [PubMed: 15514025]
- [102]. Nguyen TT, Pham M, Goo NS, Development of a Peristaltic Micropump for Bio-Medical Applications Based on Mini LIPCA, *J. Bionic Eng* 5 (2008) 135–141. 10.1016/S1672-6529(08)60017-7.
- [103]. Trenkle F, Haeberle S, Zengerle R, Normally-closed peristaltic micropump with re-usable actuator and disposable fluidic chip, *Sensors Actuators, B Chem.* 154 (2011) 137–141. 10.1016/j.snb.2009.12.069.
- [104]. Tanaka Y, A peristaltic pump integrated on a 100% glass microchip using computer controlled piezoelectric actuators, *Micromachines.* 5 (2014) 289–299. 10.3390/mi5020289.
- [105]. Jeong OC, Konishi S, Fabrication and drive test of pneumatic PDMS micro pump, *Sensors Actuators, A Phys.* 135 (2007) 849–856. 10.1016/j.sna.2006.09.012.
- [106]. Cole MC, Desai AV, Kenis PJA, Two-layer multiplexed peristaltic pumps for high-density integrated microfluidics, *Sensors Actuators, B Chem.* 151 (2011) 384–393. 10.1016/j.snb.2010.07.012.
- [107]. Berkes F, Davidson–Hunt IJ, Communities and social enterprises in the age of globalization, *J. Enterprising Communities People Places Glob. Econ* 1 (2007) 209–221. 10.1108/17506200710779521.
- [108]. Lee YS, Bhattacharjee N, Folch A, 3D-printed Quake-style microvalves and micropumps, *Lab Chip.* 18 (2018) 1207–1214. 10.1039/c8lc00001h. [PubMed: 29553156]

- [109]. Au AK, Bhattacharjee N, Horowitz LF, Chang TC, Folch A, 3D-printed microfluidic automation, *Lab Chip*. 15 (2015) 1934–1941. 10.1039/c5lc00126a. [PubMed: 25738695]
- [110]. Unger MA, Chou HP, Thorsen T, Scherer A, Quake SR., Monolithic microfabricated valves and pumps by multilayer soft lithography, *Science* (80-.). 288 (2000) 113–116. 10.1126/science.288.5463.113.
- [111]. Huang S-B, Wu M-H, Cui Z, Cui Z, Lee G-B, A membrane-based serpentine-shape pneumatic micropump with pumping performance modulated by fluidic resistance, *J. Micromechanics Microengineering* 18 (2008) 045008. 10.1088/0960-1317/18/4/045008.
- [112]. Teymoori MM, Abbaspour-Sani EA, A novel electrostatic micromachined pump for drug delivery systems, *ICONIP '02. Proc. 9th Int. Conf. Neural Inf. Process. Comput. Intell. E-Age (IEEE Cat. No.02EX575)* (2002) 105–109. 10.1109/SMELEC.2002.1217785.
- [113]. Teymoori MM, Abbaspour-Sani E, Design and simulation of a novel electrostatic peristaltic micromachined pump for drug delivery applications, *Sensors Actuators, A Phys.* 117 (2005) 222–229. 10.1016/j.sna.2004.06.025.
- [114]. Judy J, Tamagawa T, Polla DL, Surface-machined micromechanical membrane pump, [1991] *Proceedings. IEEE Micro Electro Mech. Syst* (1991) 182–186. 10.1109/MEMSYS.1991.114792.
- [115]. Patrascu M, Gonzalo-Ruiz J, Goedbloed M, Brongersma SH, Crego-Calama M, Flexible, electrostatic microfluidic actuators based on thin film fabrication, *Sensors Actuators, A Phys.* 186 (2012) 249–256. 10.1016/j.sna.2012.03.006.
- [116]. Kim H, Astle AA, Najafi K, Bernal LP, Washabaugh PD, A fully integrated high-efficiency peristaltic 18-stage gas micropump with active microvalves, in: *Proc. IEEE Int. Conf. Micro Electro Mech. Syst, 2007*: pp. 131–134. 10.1109/memsys.2007.4433033.
- [117]. Lee S, Yee SY, Besharatian A, Kim H, Bernal LR, Najafi K, Adaptive gas pumping by controlled timing of active microvalves in peristaltic micropumps, (2009) 2294–2297.
- [118]. Astle AA, Kim HS, Bernal LP, Najafi K, Washabaugh PD, Theoretical and experimental performance of a high frequency gas micropump, *Sensors Actuators A Phys.* 134 (2007) 245–256. 10.1016/J.SNA.2006.06.027.
- [119]. Besharatian A, Kumar K, Peterson RL, Bernal LP, Najafi K, A scalable, modular, multi-stage, peristaltic, electrostatic gas micro-pump, *Proc. IEEE Int. Conf. Micro Electro Mech. Syst* (2012) 1001–1004. 10.1109/MEMSYS.2012.6170183.
- [120]. Guo S, Sun X, Ishii K, Guo J, SMA actuator-based novel type of peristaltic micropump, *Proc. 2008 IEEE Int. Conf. Inf. Autom. ICIA 2008* (2008) 1620–1625. 10.1109/ICINFA.2008.4608263.
- [121]. Sassa F, Al-Zain Y, Ginoza T, Miyazaki S, Suzuki H, Miniaturized shape memory alloy pumps for stepping microfluidic transport, *Sensors Actuators, B Chem.* 165 (2012) 157–163. 10.1016/j.snb.2011.12.085.
- [122]. Sun X, Hao Y, Guo S, Ye X, Yan X, The development of a new type of compound peristaltic micropump, *2008 IEEE Int. Conf. Robot. Biomimetics, ROBIO 2008* (2008) 698–702. 10.1109/ROBIO.2009.4913086.
- [123]. Richter A, Klatt S, Paschew G, Klenke C, Micropumps operated by swelling and shrinking of temperature-sensitive hydrogels, *Lab Chip*. 9 (2009) 613–618. 10.1039/B810256B. [PubMed: 19190798]
- [124]. Folta J. a., Raley NF, Hee EW, Design, fabrication and testing of a miniature peristaltic membrane pump, *Tech. Dig. IEEE Solid-State Sens. Actuator Work* (1992). 10.1109/SOLSEN.1992.228296.
- [125]. Knight M, House J, Design, fabrication, and test of a peristaltic micropump, *Microsyst. Technol* 10 (2004) 426–431. 10.1007/s00542-004-0427-y.
- [126]. Tuantranont A, Mamanee W, Lomas T, Porntheerapat N, Afzulpurkar NV, Wisitsoraat A, A three-stage thermopneumatic peristaltic micropump for PDMS-based micro/nanofluidic systems, *2007 7th IEEE Int. Conf. Nanotechnol. - IEEE-NANO 2007, Proc* (2007) 1203–1206. 10.1109/NANO.2007.4601399.
- [127]. Mamanee W, a Tuantranont N V Afzulpurkar, N. Porntheerapat, S. Rahong, a Wisitsoraat, PDMS Based Thermopneumatic Peristaltic Micropump for Microfluidic Systems, *J. Phys. Conf. Ser* 34 (2006) 564–569. 10.1088/1742-6596/34/1/093.

- [128]. Jeong OC, Park SW, Yang SS, Pak JJ, Fabrication of a peristaltic PDMS micropump, *Sensors Actuators, A Phys.* 123–124 (2005) 453–458. 10.1016/j.sna.2005.01.035.
- [129]. Chia BT, Liao HH, Yang YJ, A novel thermo-pneumatic peristaltic micropump with low temperature elevation on working fluid, *Sensors Actuators, A Phys.* 165 (2011) 86–93. 10.1016/j.sna.2010.02.018.
- [130]. Ogden S, Klintberg L, Thornell G, Hjort K, Bodén R, Review on miniaturized paraffin phase change actuators, valves, and pumps, *Microfluid. Nanofluidics* 17 (2014) 53–71. 10.1007/s10404-013-1289-3.
- [131]. Johnson DG, Borkholder DA, Towards an implantable, low flow micropump that uses no power in the blocked-flow state, *Micromachines.* 7 (2016). 10.3390/mi7060099.
- [132]. Saren A, Smith AR, Ullakko K, Integratable magnetic shape memory micropump for high-pressure, precision microfluidic applications, *Microfluid. Nanofluidics* 22 (2018) 1–10. 10.1007/s10404-018-2058-0.
- [133]. Wu C, Zhang Q, Fan X, Song Y, Zheng Q, Smart magnetorheological elastomer peristaltic pump, *J. Intell. Mater. Syst. Struct* 30 (2019) 1084–1093. 10.1177/1045389X19828825.
- [134]. Yamatsuta E, Ping Beh S, Uesugi K, Tsujimura H, Morishima K, A Micro Peristaltic Pump Using an Optically Controllable Bioactuator, *Engineering.* 5 (2019) 580–585. 10.1016/j.eng.2018.11.033.
- [135]. Bandopadhyay A, Tripathi D, Chakraborty S, Electroosmosis-modulated peristaltic transport in microfluidic channels, *Phys. Fluids* 28 (2016). 10.1063/1.4947115.
- [136]. Forouzandeh F, Ahamed NN, Hsu M-C, Walton JP, Frisina RD, Borkholder DA, A 3D-Printed Modular Microreservoir for Drug Delivery, *Micromachines.* 11 (2020) 648. 10.3390/mi11070648.
- [137]. Cantwell CT, Wei P, Ziaie B, Rao MP, Modular reservoir concept for MEMS-based transdermal drug delivery systems, *J. Micromechanics Microengineering* 24 (2014). 10.1088/0960-1317/24/11/117001.



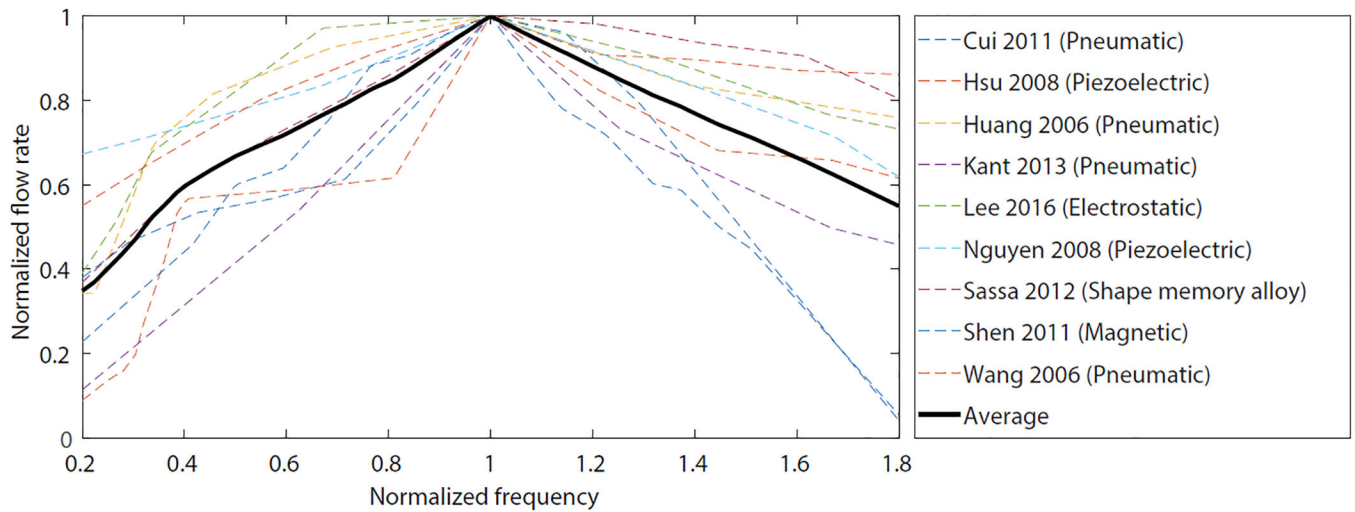


**Figure 1.**

Typical flow rate versus operating frequency ( $f$ ) for nine PMPs with various actuation methods. The flow rates and frequencies are normalized to the corresponding values at the maximum flow rate, where flow rate value of '1' shows maximum flow rate ( $Q_{max}$ ) and operating frequency of '1' reflects frequency at which the maximum flow rate occurs ( $f_{Q_{max}}$ ). The bold black line shows the average of all curves, demonstrating a trend of relatively linear dependence of flow rate to  $f$ , followed by a maximum flow rate (at  $f_{Q_{max}}$ ), and then the flow rate decreases with a further increase in  $f$ .

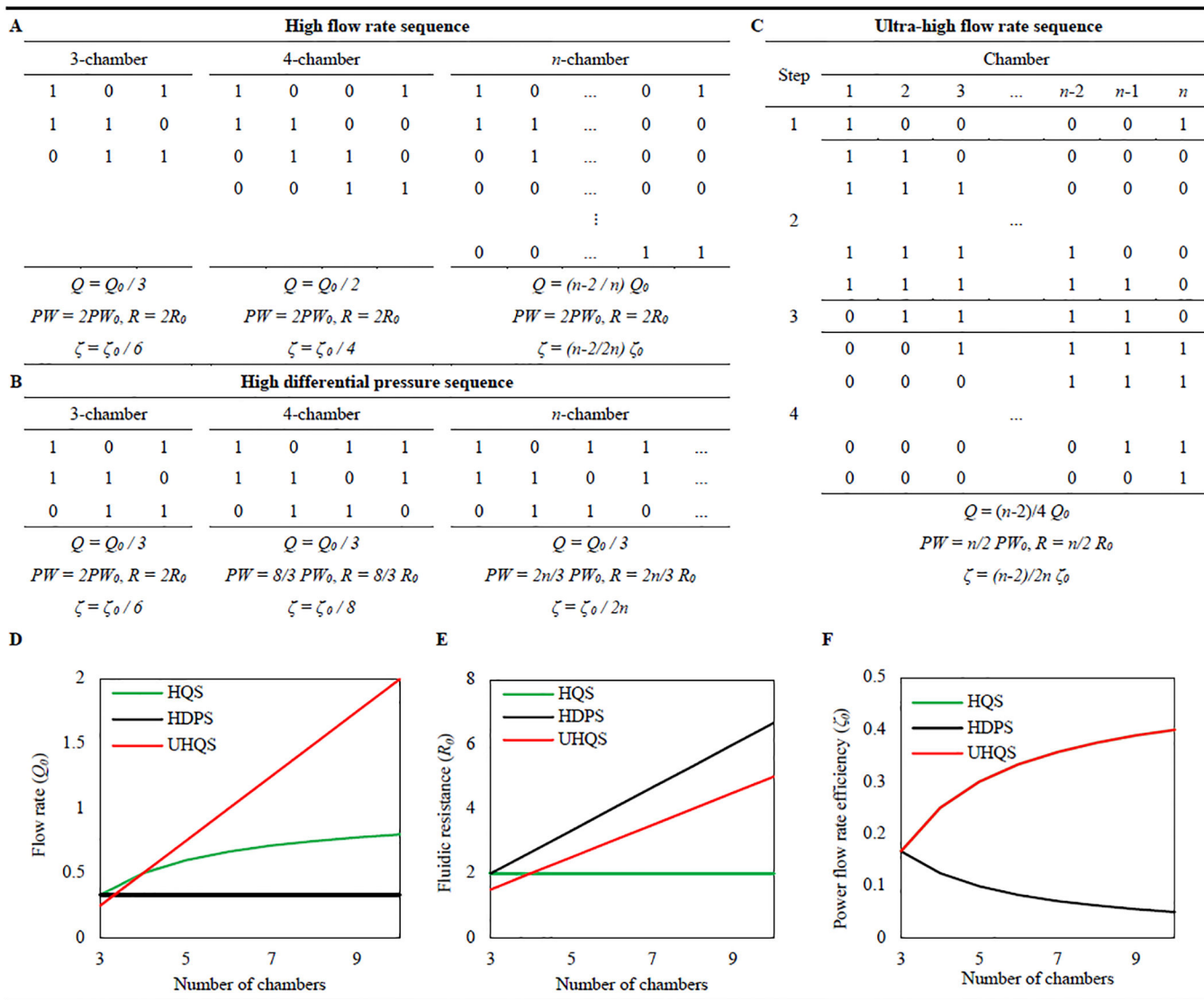


**Figure 2.** Definition and comparison of three sequences for peristaltic micropumps. (A) High flow rate sequence for 3, 4, and  $n$  chambers (B) High differential pressure sequence for 3, 4, and  $n$  chambers (C) Ultra-high flow rate sequence for  $n$  chambers. (D) Comparison of flow rate of the three sequences versus number of chambers. (E) Fluidic resistances for the three sequences versus number of chambers. (F) comparison of power flow rate efficiency for the three sequences. The values of HQS and UHQS overlap. Values presented for flow rate ( $Q$ ) in terms of stroke volume per step time ( $Q_0 = V_{st}/T_0$ ), fluidic resistance ( $R$ ) in terms of individual chamber fluidic resistance ( $R_0$ ), power consumption ( $PW$ ) in terms of individual chamber power consumption ( $PW_0$ ), and power flow rate efficiency ( $\zeta$ ) in terms of  $\zeta_0 = Q_0/PW_0$

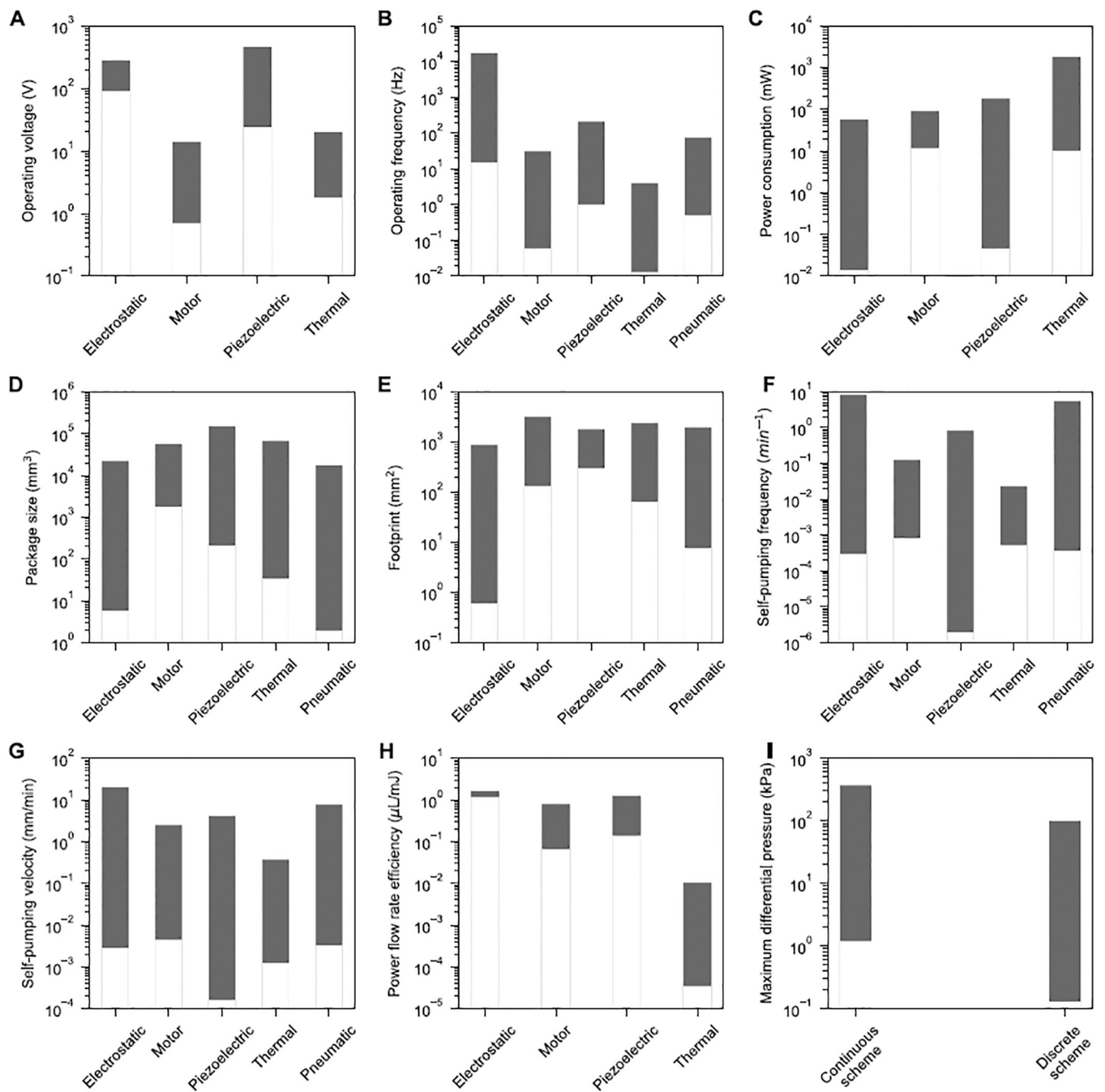


**Figure 3.**

Comparison of various actuation methods used for PMPs based on their (A) Operating voltage (B) Operating frequency (C) Power consumption (D) Package size (E) On-chip footprint (F) Self-pumping frequency (G) Self-pumping velocity and (H) Power flow rate efficiency. (I) Maximum differential pressure for continuous and discrete -scheme PMPs. Performance characteristics are reported at maximum flow rate.

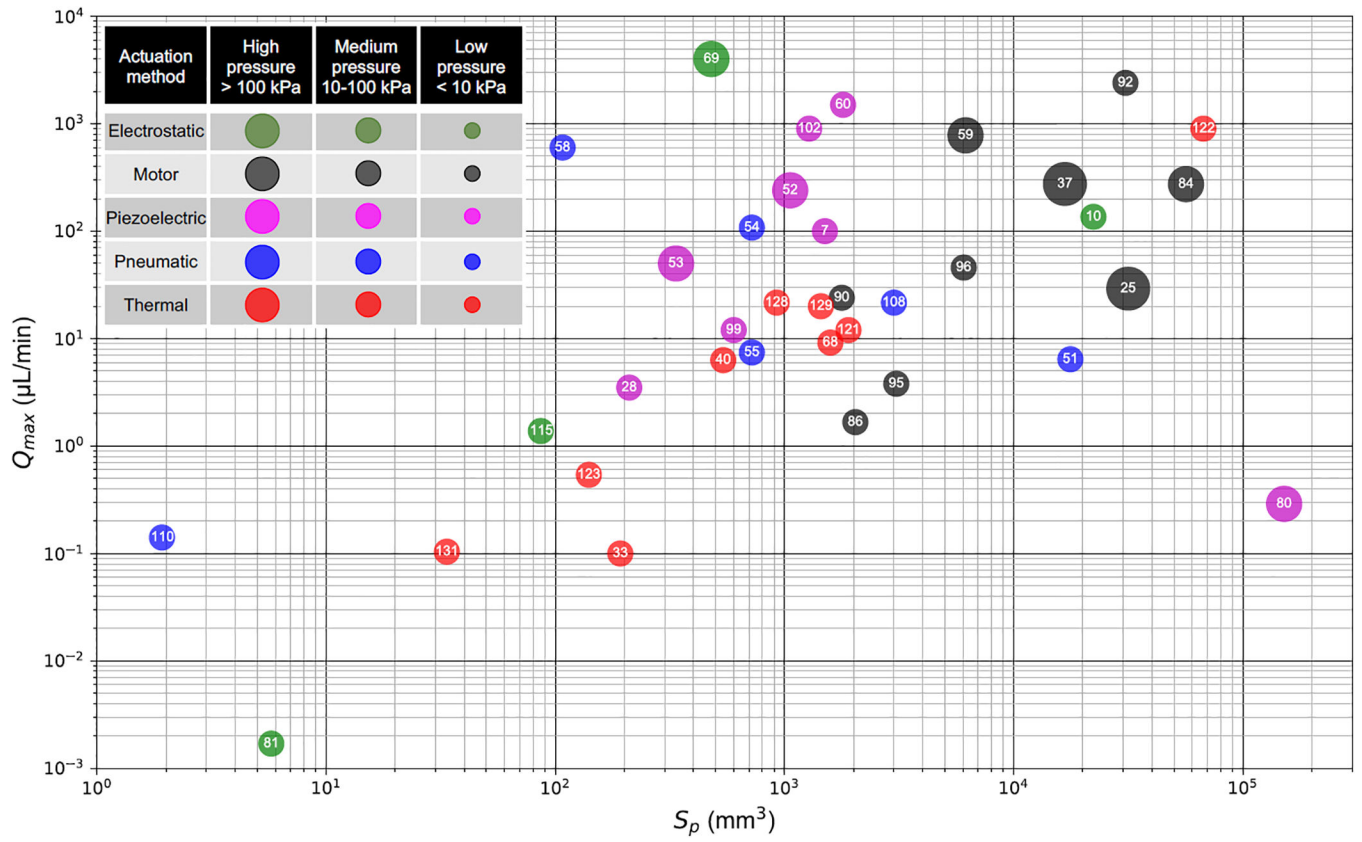


**Figure 4.** Comparison of several reported PMPs based on maximum flow rate ( $Q_{max}$ ), package size ( $S_p$ ), maximum backpressure, and actuation method. Numbers show the reference numbers.

**Table 1.**

Typical rectification methods of reciprocating mechanical micropumps.

|                |  |
|----------------|--|
| Dynamic Valves | Active (e.g., cantilever, diaphragm)                               |
|                | Passive (e.g., flip valves, check valves)                          |
| Static Valves  | Active (e.g., laser, local heating)                                |
|                | Passive (e.g., nozzle/diffuser)                                    |
| Peristalsis    | Continuous-scheme (e.g., DC motor-driven rollers on microchannels) |
|                | Discrete-scheme (e.g., multiple chamber/diaphragm configuration)   |

Author Manuscript

Author Manuscript

Author Manuscript

Author Manuscript

**Table 2.**

Categorization of different PMPs with schematic views of structures and sample operations. Discrete-channel PMPs are shown for simplification. Red arrows show actuation direction, while blue arrows show the direction of actuated fluid. The encircled number in the operation column show actuation steps for discrete-scheme PMPs. Continuous scheme PMPs do not have these numbers since they work continuously (i.e., infinite steps).

|                               | Structure | Operation | Actuators | Chambers |
|-------------------------------|-----------|-----------|-----------|----------|
| <b>Discrete-scheme PMPs</b>   |           |           |           |          |
| A                             |           |           | 3+        | 3+       |
| B                             |           |           | 2         | 2        |
| C                             |           |           | 1         | 3+       |
| <b>Continuous-scheme PMPs</b> |           |           |           |          |
| D                             |           |           | 1         | 1        |
| E                             |           |           | 1+        | 1        |

Author Manuscript

Author Manuscript

Author Manuscript

Author Manuscript

**Table 3.**

Typical advantages and disadvantages of different major actuation methods used in PMPs.

| Actuation method   | Advantages   | Disadvantages   |
|--|--|---|
| Electrostatic  | Fast response  | High operating voltage                                |
|  | Simple-to-control stroke                                 | Small stroke  |
|  | Low power consumption                                    | Electrolysis (for polar working fluids)               |
|  | Planar structure   |   |
|  | Small footprint and size                                 |   |
| Motor  | Low operating voltage                                    | Complex external mechanism for handling rotary motion |
|  | Large stroke   | Non-planar structure                                  |
|  | Peristalsis-friendly                                     | Relatively large                                      |
|  | Flexibility to couple to various transmission mechanisms |   |
| Piezoelectric  | Large actuation force                                    | High operating voltage                                |
|  | Fast response  | Small stroke  |
|  | Simple structure   | Complex and bulky driving circuit                     |
|  | Planar structure   |   |
| Pneumatic  | Large stroke   | Slow response   |
|  | Simple-to-control actuation force                        | Non-planar structure                                  |
|  | Small footprint  | External compressed air and control valves required   |
|  | Soft-lithography-friendly                                | Not portable  |
| Thermal (Thermopneumatic Phase-change Shape memory alloy Hydrogel) | Low operating voltage                                    | Slow response   |
|  | Large stroke   | High power consumption                                |
|  | Large actuation force                                    | Temperature elevation in working fluid                |
|  | Planar structure   |   |
|  | Small footprint and size                                 |   |
|  | Simple driving circuit                                   |   |

**Table 4.**

Summary of significant PMPs with their experimental output.

| Actuation method     | Transmission              | Actuation scheme | Chambers       | Fluid channel | $V_{Qmax}$ (V) | $P_{max}$ (kPa) | $Q_{max}$ ( $\mu\text{L}/\text{min}$ ) | $f_{Qmax}$ (Hz) | $PW_{Qmax}$ (mW) | $S_p$ ( $\text{mm}^3$ ) | $A_p$ ( $\text{mm}^2$ ) | Application               | Ref.  |
|----------------------|---------------------------|------------------|----------------|---------------|----------------|-----------------|--|-----------------|------------------|-------------------------|-------------------------|---------------------------|-------|
| <b>Electrostatic</b> | -                         | D                | 3              | D             | 280            | 1.6             | 0.0017                                 | 20              | -                | 6                       | 1                       | $\mu\text{TAS}$           | [81]  |
|                      | -                         | D                | 3              | D             | 150            | -               | 1.38                                   | 400             | 0.014            | 86                      | 128                     | LOC                       | [115] |
|                      | -                         | D                | 18             | D             | 200            | 17.5            | 4000                                   | 17000           | 57               | 479                     | 197                     | GC                        | [69]  |
|                      | -                         | D                | 4              | D             | 90             | -               | 136                                    | 15              | -                | 22264                   | 880                     | GC                        | [10]  |
| <b>Motor</b>         | cam/follower              | D                | 7              | C             | 1.55           | -               | 1.67                                   | -               | -                | 2036                    | 372                     | DD                        | [86]  |
|                      | cam/follower              | C                | 1              | C             | 3              | 48              | 780                                    | -               | 90               | 6160                    | 770                     | General                   | [59]  |
|                      | cam/follower              | C                | 1              | D             | 12             | 36              | 274                                    | 2.83            | -                | 56448                   | 160                     | POC, $\mu\text{Fluidics}$ | [84]  |
|                      | cam/follower              | C                | 1              | C             | 5              | 120             | 275                                    | 0.2             | 50               | 16717                   | 380                     | Insulin delivery          | [37]  |
|                      | magnetic                  | C                | 1              | D             | 14             | 1.2             | 45.8                                   | 0.13            | 11.6             | 6048                    | 432                     | LOC                       | [96]  |
|                      | magnetic                  | D                | 3              | D             | 1              | 0.33            | 24                                     | 31              | -                | 2960                    | 132                     | DD                        | [90]  |
|                      | magnetic                  | C                | 1              | D             | -              | -               | 3.8                                    | 0.13            | -                | 3072                    | 256                     | LOC                       | [95]  |
|                      | magnetic                  | D                | 1              | D             | 0.7            | 6.6             | 2400                                   | 12              | 50               | 30720                   | 960                     | POC, $\mu\text{Fluidics}$ | [92]  |
| <b>Piezoelectric</b> | roller                    | C                | 1              | C             | 12             | 370             | 29.2                                   | 0.06            | -                | 31588                   | 3200                    | LOC                       | [25]  |
|                      | -                         | D                | 3 <sup>†</sup> | D             | 100            | 5.9             | 100                                    | 15              | -                | 1500                    | 750                     | Insulin delivery          | [7]   |
|                      | -                         | D                | 3              | D             | 120            | 3.3             | 12                                     | 10              | -                | 600                     | 600                     | $\mu\text{TAS}$ , LOC     | [99]  |
|                      | -                         | D                | 2              | D             | 160            | 100             | 50                                     | 5               | -                | 336                     | 336                     | Implantable DD            | [53]  |
|                      | -                         | D                | 3              | D             | 160            | 1.8             | 900                                    | 60              | 45               | 1280                    | 320                     | Biomedical                | [102] |
|                      | -                         | D                | 3              | D             | 180            | 35.3            | 0.29                                   | 30              | -                | 151280                  | 1800                    | -                         | [80]  |
|                      | <i>PtP</i> convertor      | C                | 1              | D             | 140            | -               | 1500                                   | 210             | 180              | 1800                    | 360                     | $\mu\text{TAS}$           | [60]  |
|                      | <i>PtP</i> convertor      | C                | 1              | D             | 460            | 36              | 240                                    | 75              | -                | 1058                    | 529                     | -                         | [52]  |
| <b>Pneumatic</b>     | -                         | D                | 3 <sup>†</sup> | D             | 24             | 3.2             | 3.5                                    | 1               | 0.05             | 210                     | 300                     | DD                        | [28]  |
|                      | $\mu\text{Channel}$       | D                | 3              | D             | -              | -               | 0.141                                  | 75              | -                | 2                       | 8                       | $\mu\text{Fluidics}$      | [110] |
|                      | $\mu\text{Channel}$       | D                | 2              | D             | -              | 0.17            | 6.42                                   | 0.5             | -                | 17663                   | 1963                    | LOC                       | [51]  |
|                      | $\mu\text{Channel-delay}$ | D                | 3              | D             | -              | 0.16            | 108                                    | 10              | -                | 720                     | 600                     | $\mu\text{TAS}$           | [54]  |
|                      | $\mu\text{Channel-delay}$ | D                | 7              | D             | -              | 0.13            | 7.43                                   | 9               | -                | 720                     | 600                     | $\mu\text{TAS}$           | [55]  |
|                      | $\mu\text{Channel-delay}$ | D                | 3              | D             | -              | 0.79            | 600                                    | 30              | -                | 108                     | 77                      | Biomedical                | [58]  |
|                      | $\mu\text{Channel}$       | D                | 3              | C             | -              | 1.4             | 21.6                                   | 6.7             | -                | 3000                    | 600                     | $\mu\text{Fluidics}$      | [108] |
| <b>Thermal-HG</b>    | -                         | D                | 5              | D             | 7              | -               | 0.54                                   | 0.013           | 260              | 140                     | 350                     | General                   | [123] |
|                      | -                         | D                | 4              | D             | -              | -               | 0.1                                    | 0.083           | 10.1             | 34                      | 84                      | DD                        | [131] |
| <b>Thermal-PC</b>    | -                         | D                | 3              | C             | 1.8            | -               | 0.1                                    | 0.21            | -                | 192                     | 64                      | DD                        | [33]  |
|                      | -                         | D                | 3              | C             | 2.5            | -               | 900                                    | 0.3             | 1440             | 67200                   | 2400                    | Biomedical                | [122] |



| Actuation method  | Transmission | Actuation scheme | Chambers | Fluid channel | $V_{Qmax}$ (V) | $P_{max}$ (kPa) | $Q_{max}$ ( $\mu\text{L}/\text{min}$ ) | $f_{Qmax}$ (Hz) | $PW_{Qmax}$ (mW) | $S_p$ ( $\text{mm}^3$ ) | $A_p$ ( $\text{mm}^2$ ) | Application               | Ref.  |
|-------------------|--------------|------------------|----------|---------------|----------------|-----------------|--|-----------------|------------------|-------------------------|-------------------------|---------------------------|-------|
| <b>Thermal-TP</b> | -            | D                | 2        | C             | -              | -               | 12                                     | 0.125           | 500              | 1901                    | 704                     | $\mu\text{TAS}$ , LOC     | [121] |
|                   | -            | D                | 3        | D             | -              | 3.45            | 6.3                                    | 4               | 291              | 540                     | 270                     | n/r                       | [40]  |
|                   | -            | D                | 3        | D             | 20             | -               | 21.6                                   | 2               | -                | 924                     | 231                     | LOC                       | [128] |
|                   | -            | D                | 3        | D             | 5              | 0.4             | 9.18                                   | 1.5             | 1786             | 1584                    | 288                     | Biomedical                | [68]  |
|                   | -            | D                | 3        | D             | 9              | 0.49            | 20                                     | 1.2             | -                | 1440                    | 288                     | POC, $\mu\text{Fluidics}$ | [129] |

D: Discrete, C: Continuous,  $\mu\text{TAS}$ : Micro-total analysis, LOC: Lab-on-a-chip, GC: Gas chromatography, DD: Drug delivery, POC: Point-of-care diagnostics,

<sup>†</sup>: Chambers at inlet and outlet, PtP: Perpendicular to parallel.